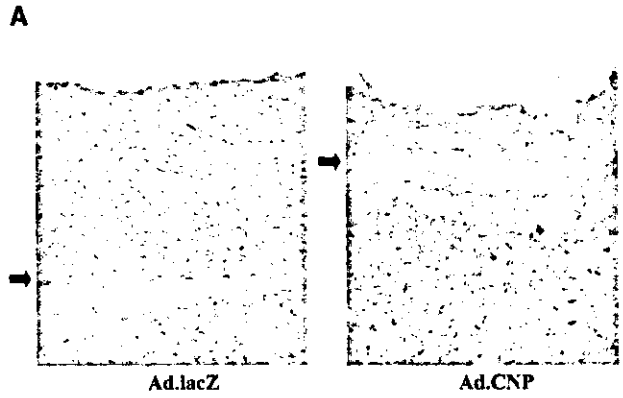

A, Immunohistochemical analysis of CNP expression in rabbit grafted veins infected with either control *Ad.LacZ* (left) or *Ad.CNP* (right). Arrows indicate internal elastic lamina. Blue shows CNP. B, Representative macroscopic appearance of rabbit grafted jugular veins 14 days (left) and 28 days (right) after operation. Reendothelialized area is not stained by Evans blue and appears white. Thrombi are brown.

We also constructed an adenoviral vector, *Ad.lacZ* overexpressing *Escherichia coli* β-galactosidase (*lacZ*) gene.

Animal Preparation

Male Japanese white rabbits weighing between 2.5 and 3.5 kg underwent unilateral interposition carotid jugular vein grafts, as previously reported.[12] The right jugular vein was cannulated with a 24-gauge catheter. A 2F Fogarty balloon catheter was inserted, and after the balloon was inflated with 0.2 mL of air, the intima of the jugular vein was denuded by three passages of the catheter. The vein was ligated again just above the incision, and 150 μL of sorbitol-added lactated Ringer's saline (Otsuka Pharmaceutical) containing 5×10^8 PFU of *Ad.CNP* (n=10) or *Ad.lacZ* (n=10) was infused and incubated for 30 minutes. Internal pressure of the vein was ~30 mm Hg. The vein segment was harvested and anastomosed into the ipsilateral carotid artery in a reverse end-to-end fashion. Fourteen or 28 days after the procedure, the animals were killed by overdose of sodium pentobarbital.

Thirty minutes before the animals were killed, 3 mL of 1.5% Evans blue dye (Sigma Chemical Co) was infused through the ear vein. The grafted carotid arteries were harvested after perfusion fixation with 10% phosphate-buffered formalin.

Planimetric Analysis of Reendothelialization and Vessel Morphometry

The grafts were incised longitudinally and photographed for planimetric analysis of the reendothelialized area. The area that was stained blue was interpreted as representing areas still denuded.

Potentiation of Wounded HCAEC Repair by CNP and ANP

	Cumulative Cell Number				
	Distance Moved, ×125 μm				
Treatment	1	2	3	4	5
(n=8)					
Control (2.5% FCS)	60±3	107±7	142±10	159±13	163±14
CNP (10^{-10} mol/L)	72±6	134±9*	177±12*	200±16*	207±17*
ANP (10^{-10} mol/L)	77±5*	134±10*	175±11*	200±13*	209±13*
C-ANF[4–23] (10^{-10} mol/L)	66±6	115±9	141±12	148±13	150±14
VEGF (10 ng/mL)	98±4*	180±8*	240±11*	267±16*	272±17*
(n=9)					
Control (1% FCS)	57±2	80±3	93±4	94±4	94±4
CNP					
10^{-15} mol/L	64±4	91±4	106±4	109±5*	109±5*
10^{-13} mol/L	78±4*	116±5*	133±7*	136±7*	136±7*
10^{-11} mol/L	86±4*	119±4*	139±4*	146±4*	146±4*
10^{-9} mol/L	68±3	91±4	98±5	99±5	99±5
10^{-7} mol/L	62±4	84±6	90±6	90±6	90±6

Values are cumulative cell numbers shown as mean±SEM.
*$P<0.05$ vs corresponding controls.

Computerized planimetry (NIH Image version 1.61) was used for the analysis. The areas of both reendothelialization and thrombosed vessel wall were calculated as the ratio to the total luminal area in the whole graft. The vessels were then stained with elastin/van Gieson. Intimal thickness and medial thickness were measured by the same digital planimetry in at least 3 histological sections from each graft and at 5 equally divided segments in each section. Immunostaining for CNP was performed with our specific CNP monoclonal antibody, as previously reported.[8] cGMP levels in grafted veins were determined as previously reported.[4]

Wound Assays

Confluent monolayers of human coronary endothelial cells (HCAECs; Clonetics; Walkersville, Md) were grown to confluency in 6-well plates, and half of the cells were scraped off and the cultures were further incubated in MCDB-131 medium containing 1% or 2.5% FCS.[13] Control cultures and cultures containing vascular endothelial growth factor (VEGF 165; Sigma) (10 ng/mL), ANP (human ANP [1–28]) (10^{-10} mol/L), CNP (CNP-22; Peptide Institute) (10^{-15} to 10^{-7} mol/L), and des-(Gln[18], Ser[19], Gly[20], Leu[21], Gly[22])-ANP (4–23) amide (C-AMF [4–23]); Sigma) (10^{-10} mol/L) were incubated at 37°C for 3 days. Migration and proliferation were quantified by counting the number of cells in 5 successive 125-μm sections from the wound edge. Effects of CNP on cell proliferation were also evaluated, as previously reported.[11]

Statistical Analysis

All values are expressed as mean±SEM. Factorial ANOVA followed by Bonferroni/Dunn was used to determine significant differences in multiple comparisons.

Results

Neointimal Thickening

In *Ad.CNP*-treated grafts, CNP immunostaining was detected both in the intima and the media, as shown in the Figure (A). The tissue level of cGMP was significantly higher in *Ad.CNP*-treated grafts (4.58±0.23 fmol/mg) than *Ad.lacZ*-treated grafts (0.89±0.41 fmol/mg, n=4, $P<0.05$). *Ad.lacZ*-treated grafts showed considerable neointimal thickening by 28 days (the ratio of intima to media: 14 days, 1.22±0.13; 28 days, 1.48±0.12). On the other hand, in the *Ad.CNP*-treated group, neointimal thickening was significantly suppressed (14 days, 0.43±0.11; 28 days, 0.47±0.06; $P<0.05$ versus *Ad.lacZ*-treated group).

Reendothelialization

The Figure (B) shows Evans blue dye staining of the adenovirus-infected vein grafts. The endothelialized areas in *Ad.lacZ*-infected grafts were 0.30±0.14 on day 14 and 0.46±0.08 on day 28. In contrast, in the *Ad.CNP*-infected group, 0.81±0.05 on day 14 and 0.96±0.01 of the whole intimal area on day 28 were reendothelialized. Thus, CNP overexpression in grafted rabbit jugular veins remarkably accelerated reendothelialization ($P<0.05$ both on day 14 and day 28 versus the *Ad.LacZ*-infected group).

Thrombotic Occlusion and Mural Thrombus Formation

In the *Ad.LacZ*-infected group, mural thrombi were formed in 4 of 5 rabbits by 14 days and 5 of 5 (with total thrombotic occlusion of one case) by 28 days. In contrast, in the *Ad.CNP*-infected group, no thrombus formation was detected by 14 days, but by 28 days, thrombus formation was detected in 1 of 5 rabbits (Figure, B). The mural thrombus area was smaller in *Ad.CNP*-infected grafts than in *Ad.LacZ*-infected grafts (14 days: 0 versus 0.20±0.09; 28 days: 0.01±0.01 versus 0.31±0.17).

Promotion of Wound Repair of Cultured Endothelial Cells

The Table depicts the effect of CNP on the repair process of wounded cultured HCAECs. VEGF as the positive control significantly promoted the wound healing of HCAECs. The administration of CNP significantly potentiated this wound

repair process. ANP at the same concentration also exerted the similar action, whereas C-ANF (4–23), which is the agonist for the clearance receptor of natriuretic peptides and lacks the potency to stimulate cGMP production,[5] had no significant effect. As shown in the Table, the effect of CNP on promotion of wound repair was dose-dependent within lower doses (10^{-5} to 10^{-11} mol/L). Higher doses of CNP (10^{-9} to 10^{-7} mol/L) had no significant effect. The same pattern of CNP effect was observed in cell number increase, which was inhibited by a cGMP-dependent protein kinase inhibitor (RP8-CPT-cGMP) (data not shown).

Discussion

In reversed autologous vein bypass grafting of the common carotid artery in rabbits, the present study demonstrates that CNP overexpression in the vein graft caused not only suppression of intimal thickening but also acceleration of reendothelialization with less thrombus formation, which indicates that CNP gene transfer at the time of vein grafting prevents the sequence of vein graft failure, for example, to reduce early thrombosis, reduce intima formation, and prevent atherosclerosis.

In this study, we observed early reendothelialization in *Ad.CNP*-infected grafts. Furthermore, in the in vitro wound assay, both CNP and ANP significantly promoted the wound-repair process to a similar extent. In contrast, C-ANF (4–23), which does not stimulate cGMP production, did not exert a significant effect. These findings of ours, together with the previous report on NO,[9] indicate that elevation of cGMP production in endothelial cells promotes their migration and/or proliferation. This is the first demonstration that the gene transfer of CNP, the vasodilator and the stimulator of cGMP genesis, can accelerate reendothelialization.

This study also revealed that the vein graft infected with *Ad.CNP* was less susceptible to thrombus formation. The mechanism of suppression of thrombus formation by CNP overexpression is not clear at present. Early reendothelialization observed in this study can be one of the mechanisms. Recently, it has been demonstrated that natriuretic peptides and NO can suppress the expression of plasminogen activator inhibitor-1 or tissue factor.[10] Overexpression of CNP can also directly modulate the expression of molecules regulating blood coagulation and fibrinolysis.

This study demonstrated that gene transfer of the soluble factor CNP into the graft to prevent both early and late occlusion, with endothelial recovery, is a promising strategy to circumvent graft failure, without obvious systemic complications such as decrease of blood pressure or bleeding tendency.

References

1. Motwani JG, Topol EJ. Aortocoronary saphenous vein graft disease: pathogenesis, predisposition, and prevention. *Circulation*. 1998;97:916–931.
2. Luscher TF, Diederich D, Siebenmann R, et al. Difference between endothelium-dependent relaxations in arterial and in venous coronary bypass grafts. *N Engl J Med*. 1988;319:462–467.
3. Yang Z, von Segesser L, Bauer E, et al. Different activation of endothelial L-arginine and cyclooxygenase pathway in human internal mammary artery and saphenous vein. *Circ Res*. 1991;68:52–60.
4. Ikeda T, Itoh H, Komatsu Y, et al. Natriuretic peptide receptors in human arterial and venous coronary bypass vessels and rabbit vein grafts. *Hypertension*. 1996;27:833–837.
5. Itoh H, Pratt RE, Dzau VJ. Atrial natriuretic polypeptide inhibits hypertrophy of vascular smooth muscle cells. *J Clin Invest*. 1990;86:1690–1697.
6. Suga S, Nakao K, Itoh H, et al. Endothelial production of C-type natriuretic peptide and its marked augmentation by transforming growth factor-β: possible existence of "vascular natriuretic peptide system." *J Clin Invest*. 1992;90:1145–1149.
7. Komatsu Y, Nakao K, Itoh H, et al. Vascular natriuretic peptide. *Lancet*. 1992;340:622.
8. Naruko T, Ueda M, van der Wal AC, et al. C-type natriuretic peptide in human coronary atherosclerotic lesions. *Circulation*. 1996;94:3103–3108.
9. Ziche M, Morbidelli L, Masini E, et al. Nitric oxide mediates angiogenesis in vivo and endothelial cell growth and migration in vitro promoted by substance P. *J Clin Invest*. 1994;94:2036–2044.
10. Yoshizumi M, Tsuji H, Nishimura H, et al. Natriuretic peptides regulate the expression of tissue factor and PAI-1 in endothelial cells. *Thromb Haemost*. 1999;82:1497–1503.
11. Doi K, Itoh H, Ikeda T, et al. Adenovirus-mediated gene transfer of C-type natriuretic peptide causes G1 growth inhibition of cultured vascular smooth muscle cells. *Biochem Biophys Res Commun*. 1997;239:889–894.
12. Jeremy JY, Dashwood MR, Timm M, et al. Nitric oxide synthase and adenylyl and guanylyl cyclase activity in porcine interposition vein grafts. *Ann Thorac Surg*. 1997;63:470–476.
13. Odekon LE, Sato Y, Rifkin DM. Urokinase-type plasminogen activator mediates basic fibroblast growth factor-induced bovine endothelial cell migration independent of its proteolytic activity. *J Cell Physiol*. 1992;150:258–263.

Brief report

Effective contribution of transplanted vascular progenitor cells derived from embryonic stem cells to adult neovascularization in proper differentiation stage

Takami Yurugi-Kobayashi, Hiroshi Itoh, Jun Yamashita, Kenichi Yamahara, Hideyo Hirai, Takuya Kobayashi, Minetaro Ogawa, Satomi Nishikawa, Shin-Ichi Nishikawa, and Kazuwa Nakao

We demonstrated that Flk-1$^+$ cells derived from mouse embryonic stem (ES) cells can differentiate into both endothelial cells (ECs) and mural cells (MCs) to suffice as vascular progenitor cells (VPCs). In the present study, we investigated the importance of the stage of ES cell differentiation on effective participation in adult neovascularization. We obtained Flk-1$^+$ LacZ-expressing undifferentiated VPCs. Additional culture of these VPCs with vascular endothelial growth factor (VEGF) resulted in a mixture of ECs and MCs (differentiated VPCs). We injected VPCs subcutaneously into tumor-bearing mice. Five days after the injection, whereas undifferentiated VPCs were often detected as nonvascular cells, differentiated VPCs were more specifically incorporated into developing vasculature mainly as ECs. VPC-derived MCs were also detected in vascular walls. Furthermore, transplantation of differentiated VPCs augmented tumor blood flow in nude mice. These results indicate that a specific vascular contribution in adult neovascularization can be achieved by selective transplantation of ES cell–derived VPCs in appropriate differentiation stages, which should be the basis for vascular regeneration schemes. (Blood. 2003;101:2675-2678)

Introduction

Embryonic stem (ES) cells with totipotency and self-renewal are now highlighted as promising sources for regeneration medicine. Recently we demonstrated that ES cell-derived Flk-1$^+$ cells can differentiate into both endothelial cells (ECs) and mural cells (MCs; pericytes and vascular smooth muscle cells) and reproduce the vascular organization process.[1] Vascular endothelial growth factor (VEGF) promotes EC differentiation from vascular progenitor cells (VPCs). Vascular cells derived from Flk-1$^+$ cells can organize vessel-like structures in 3-dimensional culture. ES cell-derived Flk-1$^+$ cells can thus serve as VPCs.

To date, substantial trials on vascular regeneration using endothelial precursor/progenitor cells derived from somatic cells have been reported.[2-4] However, precise characterization of the transplanted cells or comparison of the effectiveness of cell differentiation stages to generate blood vessels has been scarce. We have established an in vitro vascular differentiation system using VPCs that can obtain ES cell–derived vascular cells at different stages of differentiation with homogeneity and in large quantities. Thus, in the present study, we examined the impact of differentiation stage differences of donor Flk-1$^+$ ES cells in transplantation on adult neoangiogenesis, to explore the potential of Flk-1$^+$ VPCs for vascular generation therapy.

Study design

Cell culture and sorting

Maintenance of CCE[5] ES cells (gift from M. J. Evans, Cambridge, United Kingdom) was as described previously.[6] To induce Flk-1$^+$ cells, ES cells were cultured on type IV collagen–coated dishes as reported previously.[6] Flk-1$^+$ VE-cadherin$^-$E-cadherin$^-$ cells were sorted by fluorescence-activated cell sorting (FACSVantage; Becton Dickinson, Bedford, MA) as described.[6,7] After 3 days of incubation on type IV collagen-coated dishes with 50 ng/mL VEGF (human $VEGF_{165}$; R & D Systems, Minneapolis, MN) in 10% fetal calf serum (FCS), cultured cells were harvested and further resorted by FACS. For serum-free culture, Flk-1$^+$ cells were incubated in SFO3 (Sanko Junyaku, Chiba, Japan) with 10 ng/mL platelet-derived growth factor-BB (PDGF-BB; Gibco BRL, Grand Island, NY) as described.[1] For detection of circulating LacZ$^+$ cells in peripheral blood by flow cytometry, we used FluoReporter LacZ flow cytometry kits (Molecular Probes, Eugene, OR).

Tumor transplantation and ES cell injection

Six- to 8-week-old nude (nu/nu) mice (SLC, Shizuoka, Japan) underwent subcutaneous transplantation of 1×10^6 C6 rat glioblastoma cells, which secrete large amounts of VEGF, in 0.1 mL phosphate-buffered saline (PBS) on right and left flanks as reported previously.[8] ES cells expressing *LacZ* gene (CCE/nLacZ) were generated as previously reported.[1] Seven days after tumor transplantation, C6 cells produced small tumors in both sides of the flank. We injected ES cell–derived VPCs in 0.1 mL PBS subcutaneously at 5 sites around the left tumor. Control (PBS only, right) and VPC-transplanted (left) tumors were excised 5 days after injection and sectioned into 50 blocks for whole-mount LacZ staining.

LDPI analysis of the tumor blood flow

We measured the ratios of VPCs transplanted (left) to control (right) tumor blood flow using a laser Doppler perfusion image (LDPI) analyzer (Moor Instruments, Devon, United Kingdom) 5 days after VPC transplantation.

From the Department of Medicine and Clinical Science, Department of Molecular Genetics, Kyoto University Graduate School of Medicine, Department of Microbiology, Kyoto Prefectural University of Medicine, Department of Pharmacology, Kyoto University Graduate School of Medicine, Kyoto, Japan; and Department of Cell Differentiation, Institute of Molecular Embryology and Genetics, Kumamoto University, Kumamoto, Japan.

Submitted June 26, 2002; accepted November 22, 2002. Prepublished online as *Blood* First Edition Paper, December 12, 2002; DOI 10.1182/blood-2002-06-1877.

Reprints: Hiroshi Itoh, Department of Medicine and Clinical Science, Kyoto University Graduate School of Medicine, 54 Shogoin Kawahara-cho, Sakyo-ku, Kyoto 606-8507 Japan; e-mail: hiito@kuhp.kyoto-u.ac.jp.

The publication costs of this article were defrayed in part by page charge payment. Therefore, and solely to indicate this fact, this article is hereby marked "advertisement" in accordance with 18 U.S.C. section 1734.

Results and discussion

Characterization of implanted ES cell–derived VPCs

Sorted Flk-1$^+$E-cadherin$^-$ cells did not express other EC (VE-cadherin, platelet-endothelial cell adhesion molecule 1 [PECAM-1], or CD34; Figure 1A-C) or MC (smooth muscle actin [SMA] or platelet-derived growth factor β [PDGF-β] receptor) markers (data not shown). We termed these cells "undifferentiated VPCs." After an additional 3 days of culture with 10% FCS and 50 ng/mL $VEGF_{165}$, Flk-1$^+$ cells differentiated into mixtures of ECs and MCs. The cells that retained Flk-1 expression (about 30%) became also positive for VE-cadherin, PECAM-1, and CD34, indicating the differentiation into ECs (Figure 1D-E). The cells that lost Flk-1 expression (about 70%) were negative for EC markers, but positive for SMA (Figure 1F-G) and other markers of differentiated vascular smooth muscle cells (smooth muscle myosin heavy chain, calponin, and SM22α; data not shown). These cell mixtures were designated "differentiated VPCs." We also sorted out a VE-cadherin$^+$ fraction of differentiated VPCs by FACS. Three-day treatment of undifferentiated VPCs with PDGF-BB resulted in selective induction of SMA$^+$ MCs, which were negative for Flk-1, VE-cadherin, and PECAM-1 (data not shown) in serum-free conditions (PDGF-BB–treated VPCs). Undifferentiated VPCs, differentiated VPCs (1×10^6 cells), VE-cadherin$^+$ fraction of differentiated VPCs (0.3×10^6 cells), or PDGF-BB–treated VPCs (0.7×10^6 cells) were implanted (Figure 1H-I) into nude mice. We also injected 0.5 to 1.0×10^6 undifferentiated and differentiated VPCs in PBS into the tail vein.

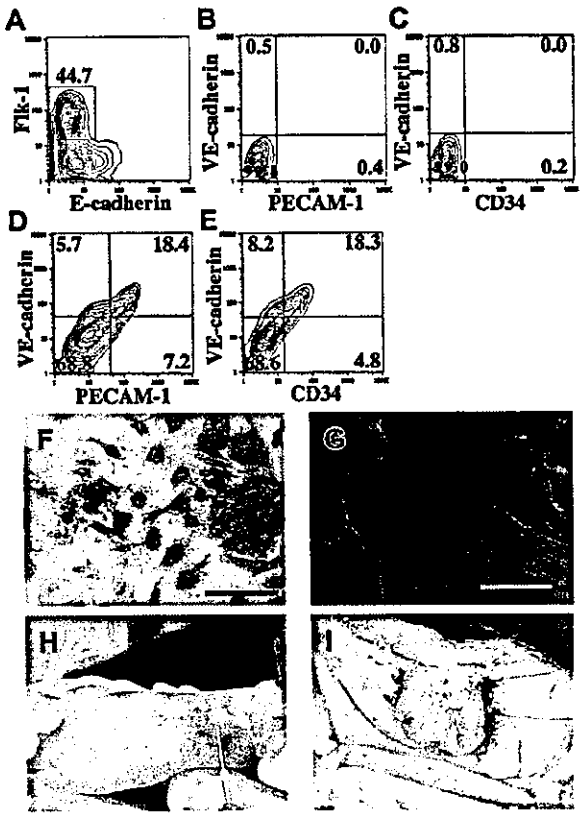

Figure 1. Characterization of injected ES cell-derived VPCs and transplantation of VPCs in tumor angiogenesis model. (A-C) Flow cytometric sorting and analysis of Flk-1$^+$ undifferentiated VPCs. CCE/nLacZ ES cells were cultured on type IV collagen-coated dishes in the absence of leukemia inhibitory factor (LIF). (A) After 4 days of differentiation, Flk-1$^+$ VPCs were sorted by flow cytometry (undifferentiated VPCs). (B-C) Flk-1$^+$ undifferentiated VPCs did not express other EC markers (VE-cadherin, PECAM-1, and CD34). (D-G) After a 3-day incubation of Flk-1$^-$ undifferentiated VPCs, differentiated VPCs were induced. Flow cytometric analysis revealed that about 30% were Flk-1$^+$VE-cadherin$^+$PECAM-1$^+$CD34$^+$ ECs and 70% were Flk-1$^-$VE-cadherin$^-$PECAM-1$^-$CD34$^-$ (D-E). (F-G) Double staining of differentiated VPCs was performed as previously reported.[1] About 70% of cells that lost Flk-1 expression were positive for SMA (brown) and surrounded PECAM-1$^+$ EC sheets (blue). (F) The expressions of PECAM-1 and SMA were exclusive for differentiated VPCs (scale bar, 100 μm). (G) Fluorescent immunostaining of Flk-1 (red) and SMA (green) revealed that they were expressed exclusively (scale bar 20 μm). (H-I) Tumor angiogenesis model of nude mice. Subcutaneous transplantation of VPCs to the growing tumor 7 days after C6 glioblastoma cell implantation was performed (H). Vascularized tumor was obtained 5 days after VPC implantation (I). Monoclonal antibody (MoAb) for murine E-cadherin (epithelial cadherin; ECCD2), Flk-1 (AVAS12), and vascular endothelial (VE)-cadherin (VECD1) have been described previously.[6,7] Fluorescein isothiocyanate (FITC)-conjugated MoAb for murine PECAM-1 (Mec13.3) and FITC-conjugated MoAb for CD34 (RAM34) were purchased from Pharmingen (San Diego, CA). MoAbs for SMA 1A4, CCA7 were obtained from Neo Markers (Fremont, CA) and ENZO Diagnostics (Farmingdale, NY).

Contribution of VPCs to the vascular component in tumor neoangiogenesis

Five days after subcutaneous injection, differentiated VPCs were demonstrated to form tubelike structures (Figure 2D), whereas undifferentiated VPCs mainly formed cell aggregates with little vascular stretch (Figure 2A). In undifferentiated VPC-injected tumors, many LacZ$^+$ cells were negative for PECAM-1 (Figure 2B-C), SMA, and CD45 (data not shown), suggesting that undifferentiated VPCs gave rise to cell types other than vascular cells. Lee et al[9] reported that unregulated VEGF expression in myocardium led to the formation of hemangioma.[10] As shown panels E and F of Figure 2, within the newly formed blood vessels with LacZ$^+$ VPC-derived cells, circulating LacZ$^-$ blood cells were clearly detected, indicating integration with the systemic circulation. We could not detect LacZ$^+$CD45$^+$ blood cells within the vessel lumen (data not shown). Circulating LacZ$^+$ blood cells were not detected by FACS analysis (data not shown). Implantation of VE-cadherin$^+$ endothelial fraction of differentiated VPCs also generated similar tube structures (Figure 2G) and contributed to the developing capillary network (Figure 2H-I). To investigate the impact of differentiation stages of ES cells for transplantation efficiency, we counted LacZ$^+$PECAM-1$^+$ cells that contributed to vascular structures (Figure 2M). Percentages of LacZ$^+$PECAM-1$^+$ cells to all LacZ$^+$ cells were 39.5% ± 14.1% (mean ± SEM; n = 3) in the undifferentiated VPC injection group, 86.9% ± 4.9% in the differentiated VPC group ($P < .05$ versus undifferentiated VPCs), and 95.3% ± 3.3% in the VE-cadherin$^+$ fraction injection group ($P < .05$ versus undifferentiated VPCs). In contrast, we did not detect LacZ$^+$ cells within the tumor after the intravenous administration of VPCs.

Interaction between ECs and MCs is essential for vascular development and maintenance of vascular integrity.[11,12] Because differentiated VPCs contained substantial numbers of SMA$^+$Flk-1$^-$ MCs, we examined the participation of the MC component to pericyte recruitment during tumor neoangiogenesis. LacZ$^+$SMA$^+$-PECAM-1$^-$ cells were detected in differentiated VPC-injected tumors (Figure 2N-O). In differentiated VPC transplantation, however, the ratio of LacZ$^+$SMA$^+$ cells to total LacZ$^+$ cells was much lower than that of LacZ$^+$PECAM-1$^+$ cells. To analyze the in vivo survival/proliferation potential of MCs, we performed selective induction of Flk-1$^-$SMA$^+$ cells from Flk-1$^+$ cells with PDGF-BB and transplanted them into the tumor. Whole-mount

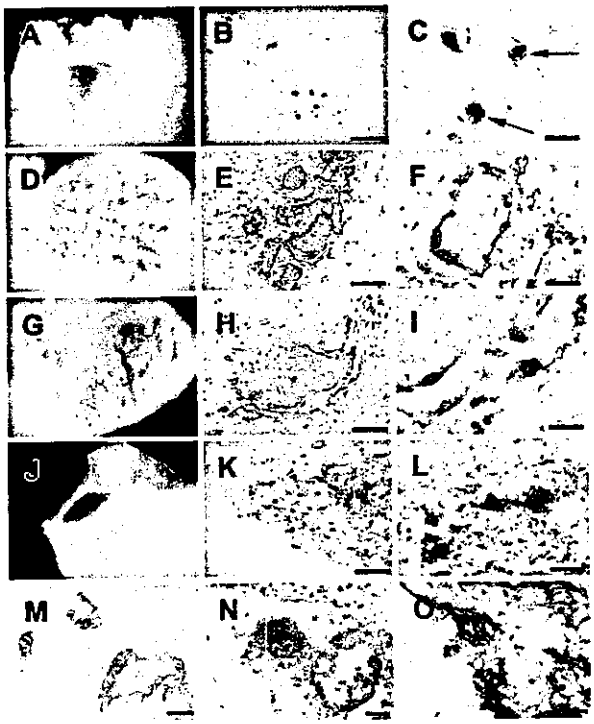

Figure 2. Contribution of ES cell-derived VPCs to tumor angiogenesis. (A,D,G,J) Whole-mount X-gal staining of the tumor. An X-gal analog, blue gal (Nacalai), was used as a substrate for staining 5 days after the injection of undifferentiated VPCs (A), differentiated VPCs (D), VE-cadherin$^+$ fraction of differentiated VPCs (G), and PDGF-BB–treated VPC (J). Undifferentiated VPCs and PDGF-BB–treated VPCs formed cell aggregates with few vascular structures (A,J). Differentiated VPCs and VE-cadherin$^+$ fraction of differentiated VPCs generated rich vascular-like networks (D,G). (B,C,E,F,H,I,K-O) Immunohistochemical staining of tumor sections. Differentiated VPCs were specifically incorporated as LacZ (blue)/PECAM-1 (brown) double-positive cells into developing vasculatures (E-F). Undifferentiated VPCs were often detected as LacZ$^-$/PECAM-1$^-$ cells (arrows; B-C). Implantation of VE-cadherin$^+$Flk-1$^-$ fraction of differentiated VPCs similarly generated specific vascular contribution as LacZ/PECAM-1 double-positive cells (H-I). Typical LacZ$^+$PECAM-1$^+$ cells (M) were observed in the differentiated VPC-injected tumor. LacZ (blue)/SMA (purple) double-positive and PECAM-1 (brown)-negative cells were also detected in the continuous sections (N-O). In the PDGF-BB–treated VPC transplantation group, some LacZ (blue)/SMA (red) double-positive cells were detected (K-L). Scale bars: panels B, E, H, K, 250 μm; panels C, F, I, L, 50 μm; panel M, 100 μm; panels N-O, 25μm.

LacZ staining of the tumor revealed that transplanted PDGF-BB–treated VPCs remained less than differentiated VPCs and formed cell aggregates (Figure 2J) similar to undifferentiated VPCs (Figure 2A). We detected some LacZ$^+$SMA$^+$ cells (Figure 2K-L) and only a few LacZ$^+$PECAM-1$^+$ cells. Most LacZ$^+$ cells were negative for either. This result indicated that although VPC-derived MCs can contribute to the MC component in tumor neoangiogenesis, the in vivo survival/proliferation potential of MCs is not high.

Transplantation of VPCs quantitatively augmented tumor blood flow in nude mice

We further investigated whether transplantation of VPCs might augment blood flow of the tumors. LDPI analyses revealed the significantly augmented ratio of differentiated VPC transplantation to control tumor blood flow (Figure 3A-B), whereas the blood flow ratios of other VPC transplantation groups were not altered. Quantification of the number of tumor blocks containing LacZ$^+$ cells demonstrated an increase of the extent of vascular expansion (Figure 3C). About 40% of tumor blocks contained LacZ$^+$ cells in the differentiated VPC transplantation group, whereas about 10% of them were seen in other VPC transplantation groups. In our protocol, no significant differences in the tumor weight were observed between control and VPC transplantation tumors among the 3 groups (data not shown).

Asahara et al[13] first demonstrated the existence of endothelial progenitor cells (EPCs) in the circulation, which are at least in part derived from bone marrow,[2] and showed that they can participate in postnatal angiogenesis after intravenous administration.[13] In our present study, intravenously administrated ES cell–derived VPCs did not contribute to tumor neoangiogenesis, suggesting that ES cell-derived VPCs might be different from somatic circulating endothelial progenitors especially in recruitment and adhesion property. EPCs were characterized as CD34$^+$Flk-1$^+$AC133$^+$ cells.[13-15] These precursors differentiated into Flk-1$^+$AC133$^-$ acetyl low-density lipoprotein (LDL) incorporated-positive ECs.[3,14-16] Our ES cell-derived VPCs are Flk-1$^+$CD34$^-$ and can differentiate into both MCs and ECs.[1] Thus, VPCs are supposed to be more premature precursors. Our results demonstrate that these undifferentiated VPCs cannot be specifically differentiated into ECs and MCs in vivo. However, differentiated VPCs, that is, VPC-derived vascular cells (ECs and MCs) at defined differentiation stages can contribute to tumor-associated vasculoangiogenesis.

The results of the present study clearly demonstrate that differentiated vascular cells derived from VPCs can contribute to generation of vascular structures in adult neoangiogenesis. Optimization of the differentiation stage of ES cells at transplantation is thus critically required to meet the challenge for cell therapy in regeneration medicine.

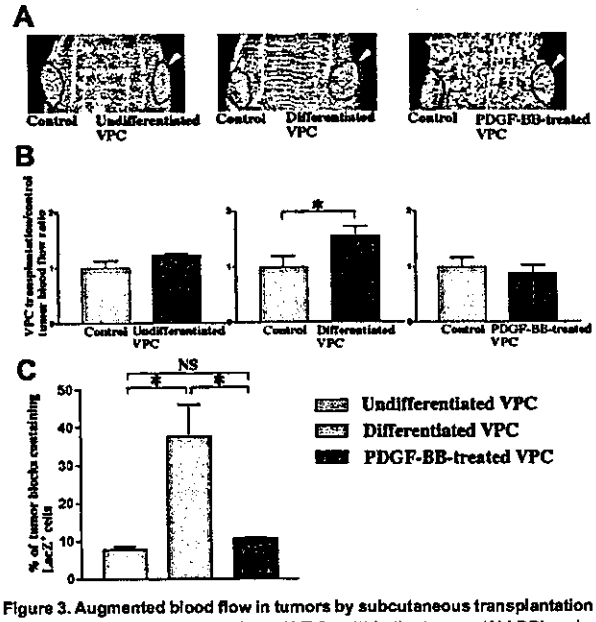

Figure 3. Augmented blood flow in tumors by subcutaneous transplantation of VPCs and expansion of transplanted VPCs within the tumor. (A) LDPI analyses of blood flow in 3 VPC transplantation groups. Bilateral generation of C6-derived tumor (black circles) and unilateral transplantation of VPCs (arrowheads) in nude mice is shown. Differentiated VPC transplantation augmented blood flow of tumor (red to white colors) compared with control, whereas undifferentiated and PDGF-BB–treated VPCs did not (blue to green colors). (B) Quantitative analyses demonstrated the significant enhancement of differentiated VPC transplantation/control tumor blood flow ratios in nude mice. Data shown (mean ± SEM) are representative of 3 experiments. *$P < .05$. (C) Percents of the number of sectioned tumor blocks containing LacZ$^+$ cells. About 40% of tumor blocks contained LacZ$^+$ cells in differentiated VPC transplantation groups, whereas about 10% of them did in other VPC transplantation groups. The number of tumor blocks containing LacZ$^+$ cells in differentiated VPC transplantation groups was significantly increased. Data shown (mean ± SEM) are representative of 3 experiments. *$P < .01$; NS, $P > .05$.

References

1. Yamashita J, Itoh H, Hirashima M, et al. Flk1-positive cells derived from embryonic stem cells serve as vascular progenitors. Nature. 2000;408: 92-96.
2. Asahara T, Takahashi T, Masuda H, et al. VEGF contributes to postnatal neovascularization by mobilizing bone marrow-derived endothelial progenitor cells. EMBO J. 1999;18:3964-3972.
3. Murohara T, Ikeda H, Duan J, et al. Transplanted cord blood-derived endothelial precursor cells augment postnatal neovascularization. J Clin Invest. 2000;105:1527-1536.
4. Kalka C, Masuda H, Takahashi T, et al. Transplantation of ex vivo expanded endothelial progenitor cells for therapeutic neovascularization. Proc Natl Acad Sci U S A. 2000;97:3422-3427.
5. Robertson E, Bradley A, Kuehn M, Evans M. Germ-like transmission of genes introduced into cultured pluripotential cells by retroviral vector. Nature. 1986;323:445-448.
6. Nishikawa SI, Nishikawa S, Hirashima M, Matsuyoshi N, Kodama H. Progressive lineage analysis by cell sorting and culture identifies Flk-1$^+$ VE-cadherin$^-$ cells at a diverging point of endothelial and hemopoietic lineages. Development.1998;125:1747-1757.
7. Hirashima M, Kataoka H, Nishikawa S, Matsuyoshi N, Nishikawa SI. Maturation of embryonic stem cells into endothelial cells in an in vitro model of vasculogenesis. Blood. 1999;93:1253-1263.
8. Kubo H, Fujiwara T, Jussila L, et al. Involvement of vascular endothelial growth factor receptor-3 in maintenance of integrity of endothelial cell lining during tumor angiogenesis. Blood. 2000;96:546-553.
9. Lee RJ, Springer ML, Blanco-Bose WE, Shaw R, Ursell PC, Blau HM. VEGF gene delivery to myocardium. Deleterious effects of unregulated expression. Circulation. 2000;102:898-901.
10. Carmeliet P. VEGF gene therapy: stimulating angiogenesis or angioma-genesis? Nat Med. 2000; 6:1102-1103.
11. Carmeliet P. Mechanisms of angiogenesis and arteriogenesis. Nat Med. 2000;6:389-395.
12. Pettersson A, Nagy JA, Brown LF, et al. Heterogeneity of angiogenic response induced in different normal adult tissues by vascular permeability factor/vascular endothelial growth factor. Lab Invest. 2000;80:99-115.
13. Asahara T, Murohara T, Sullivan A, et al. Isolation of putative progenitor endothelial cells for angiogenesis. Science. 1997;275:964-966.
14. Gehling UM, Ergun S, Schumacher U, et al. In vitro differentiation of endothelial cells from AC133-positive progenitor cells. Blood. 2000;95: 3106-3112.
15. Peichev M, Naiyer AJ, Pereira D, et al. Expression of VEGFR-2 and AC133 by circulating human CD34 (+) cells identifies a population of functional endothelial precursors. Blood.2000;95: 952-958.
16. Lin Y, Weisdorf DJ, Solovey A, Hebble RP. Origins of circulating endothelial cells and endothelial outgrowth from blood. J Clin Invest. 2000;105: 71-77.

Am J Physiol Heart Circ Physiol 284: H1388–H1397, 2003.
First published December 27, 2002; 10.1152/ajpheart.00414.2002.

Physiological concentration of atrial natriuretic peptide induces endothelial regeneration in vitro

Hyun Kook,[1] Hiroshi Itoh,[2] Bong Seok Choi,[1] Naoki Sawada,[2] Kentaro Doi,[2] Tae Ju Hwang,[1] Kyung Keun Kim,[1] Hiroshi Arai,[2] Yung Hong Baik,[1] and Kazuwa Nakao[2]

[1]*Research Institute of Medical Sciences, Chonnam National University Medical School, Gwangju 501-746, Republic of Korea; and* [2]*Department of Medicine and Clinical Science, Kyoto University Graduate School of Medicine, Kyoto 606-8507, Japan*

Submitted 20 May 2002; accepted in final form 11 December 2002

Kook, Hyun, Hiroshi Itoh, Bong Seok Choi, Naoki Sawada, Kentaro Doi, Tae Ju Hwang, Kyung Keun Kim, Hiroshi Arai, Yung Hong Baik, and Kazuwa Nakao. Physiological concentration of atrial natriuretic peptide induces endothelial regeneration in vitro. *Am J Physiol Heart Circ Physiol* 284: H1388–H1397, 2003. First published December 27, 2002; 10.1152/ajpheart.00414.2002.—Both nitric oxide (NO) and natriuretic peptides produce apoptosis of vascular smooth muscle cells. However, there is evidence that NO induces endothelial cell proliferation, which suggests that there is a difference in the response of endothelial cells to natriuretic peptides. The purpose of this study was to investigate the effect of atrial natriuretic peptide (ANP) on human endothelial cell survival. ANP within the physiological concentration (10^{-11} mol/l) induced a 52% increase in the number of human coronary arterial endothelial cells and a 63% increase in human umbilical vein endothelial cells at a low concentration of serum. The increase in cell numbers was blocked by pretreatment with RP8-CPT-cGMP (RP8), a cGMP-dependent protein kinase inhibitor, with wortmannin, an Akt/PKB inhibitor, and with PD-98059, an ERK1/2 inhibitor. In a Transwell migration test, ANP also increased the cell migration, and RP8, wortmannin, and PD-98059 blocked this increase. A wound healing assay was performed to examine the effects of ANP on regeneration in vitro. ANP increased both cell numbers and migration, but the effects were blocked by the above three kinase inhibitors. ANP increased the expression of phospho-Akt and of phospho-ERK1/2 within 1.5 h. These results suggest that ANP can potentiate endothelial regeneration by cGMP-dependent protein kinase stimulation and subsequent Akt and ERK1/2 activations.

cGMP-dependent protein kinase; Akt/protein kinase B; extracellular signal-regulated kinase 1/2

REGENERATION OF THE ENDOTHELIUM after vascular damage is an important factor that limits the development of atherogenesis (1). This process of wound repair involves different stages, which include vascular endothelial cell activation, proliferation, and migration. The growth factor-stimulated angiogenesis that forms new blood vessels from preexisting vessels (10) has been known to play a key role in initiating endothelial regeneration. However, the intracellular signal transduction mechanism remains to be clarified further.

It has been widely accepted that nitric oxide (NO) mediates the inhibition of proliferation and apoptosis in various cells including vascular smooth muscle cells. Thus the overexpression of NO synthase, producing NO, has been proposed as a therapeutic modality in vascular proliferative diseases such as neointimal hyperplasia after coronary arterial damage (43). However, the therapeutic significance of NO in such proliferative diseases of blood vessels is not a simple matter. Indeed, NO has also been implicated as a crucial signal molecule in angiogenesis. Ziche et al. (46) reported that NO donors promote endothelial cell proliferation and migration, whereas inhibitors of NO synthase suppress such effects. Furthermore, NO is known to be a mediator of VEGF, an important mitogen for vascular endothelial cells causing angiogenesis (27). More recently, cGMP-dependent protein kinase (cGK), a downstream molecule that mediates the effects of NO, has also been reported to mediate the VEGF-induced proliferation of human endothelial cells (15).

The natriuretic peptide family consists of atrial natriuretic peptide (ANP), brain natriuretic peptide (BNP), and C-type natriuretic peptide (CNP), which serve as physiological regulators of homeostasis such as body fluid control and blood pressure. They share the same intracellular signal transduction pathway regarding cGMP/cGK with NO. We demonstrated that ANP and BNP are secreted mainly from the atrium and ventricle of the heart, respectively, as cardiac hormones (28, 40), whereas CNP is secreted from endothelial cells (38) to act as an endothelium-derived relaxing peptide (22) for vascular remodeling (7, 17, 21). Natriuretic peptides, including ANP, have been suggested as having an antiangiogenic property (18).

We recently reported that in a balloon injury model of the rabbit femoral artery, overexpression of the CNP gene by adenoviral vector not only inhibits vascular smooth muscle cell proliferation but also accelerates

Address for reprint requests and other correspondence: H. Itoh, Dept. of Medicine and Clinical Science, Kyoto Univ. Graduate School of Medicine, 54 Shogoin Kawahara-cho, Sakyo-ku, Kyoto 606-8507, Japan (E-mail: hiito@kuhp.kyoto-u.ac.jp).

The costs of publication of this article were defrayed in part by the payment of page charges. The article must therefore be hereby marked "*advertisement*" in accordance with 18 U.S.C. Section 1734 solely to indicate this fact.

reendothelialization (6), demonstrating complex responses to natriuretic peptides in different types of vascular cells. Therefore, in the present study, based on the postulation that in certain conditions natriuretic peptides may also induce an increase in endothelial cell numbers and migration, we tried to characterize the mechanism of endothelial regeneration induced by ANP. Here, we demonstrate that ANP increases cell numbers and migration by activating cGK and subsequent Akt and ERK1/2 (p44/42 MAPK) pathways. The results suggest that ANP could be useful in the regeneration of endothelial cells after injury in atherosclerosis.

METHODS

Cell cultures. Human coronary arterial endothelial cells (HCAEC; Clonetics; Waltersville, MD) and human umbilical vein endothelial cells (HUVEC; Clonetics) were grown in basic media (EBM2, Clonetics) containing growth supplements (EGM2MV or EGM2).

Cell survival. Two or three days after treatment with ANP [human ANP(1–28), Peptide Institute; Suita, Japan] or Sp-8-[(4-chlorophenyl)thio]-guanosine 3′,5′-cyclic monophosphothioate triethylamine [Sp-8-*p*-CPT-cGMPs triethylamine (SP8), RBI; Natick, MA], the cells were lifted with trypsin and counted with a hemocytometer. In some experiments, Rp-8-[(4-chlorophenyl)thio]-guanosine 3′,5′-cyclic monophosphothioate triethylamine [Rp-8-*p*-CPT-cGMPs triethylamine (RP8), RBI], wortmannin (Sigma; St. Louis, MO), PD-98059 (Calbiochem; La Jolla, CA), or SB-203580 (Calbiochem) was added 20 min before ANP treatment. Because the inhibitors can affect the normal cell growth, the inhibitor alone was treated, and the cell number when the inhibitor alone was treated was regarded as 100%.

[^{3}H]thymidine incorporation. DNA synthesis was evaluated by [^{3}H]thymidine incorporation as published previously (17).

Intracellular cGMP measurements. Sixteen thousand cells were seeded into each well of 24-well plates and incubated overnight. The cells were then treated with 10^{-11} mol/l ANP and incubated for the indicated intervals. cGMP measurements were performed according to our previous report (23) with a ^{125}I radioimmunoassay kit (New England Nuclear; Boston, MA).

Cell migration assay using Transwell apparatus. Cell migration was measured using a Transwell migration apparatus (Costar; Cambridge, MA) with 8-μm pores coated with gelatin. Cells (2.4×10^5) in 120 μl EBM-0.2% BSA were loaded to the upper chamber, whereas 400 μl EBM-0.2% BSA containing ANP was loaded into the lower chamber, and incubated for 24 h at 37°C. After being stained with Diff-Quick (International Reagents; Kobe, Japan), the cells on the bottom surface were counted in six random squares of 0.5 × 0.5 mm.

Wound healing assay. The wound healing assay was performed according to a previous report (9) with some modifications. After HCAEC or HUVEC were grown to overconfluence in six-well plates, a scratch was made with a sterile cell scraper, and the starting point was marked by attaching a cover glass under the bottom of the plate; fresh culture media were supplied, and the cells were incubated for 3 days. The cells in the 10 small grids of an eyepiece micrometer (unit area: 0.1 mm height ×1 mm width, Olympus; Tokyo, Japan) just above the starting point were counted, and the next area from the wound side was then counted again. The cell numbers in the consecutive unit areas were counted and continued until no cells were observed. The cell counts were plotted using the consecutive field number as the abscissa, as shown in Fig. 4*B*, and both *x*- and *y*-axis intercepts were calculated by extrapolating the regression line.

Confocal microscopy. After treatment with ANP for 30 min, F-actin in the cells was stained with Alexa fluor 488-conjugated phalloidin (Molecular Probes; Eugene, OR) and visualized by confocal laser scanning microscopy with a Bio-Rad MRC-1024 imaging system (Hercules, CA) mounted on an Olympus Microscope (CK40) equipped with a ×60 objective lens.

Immunoblotting. After serum starvation with EBM2 containing 0.5% FBS for 24 h, HUVEC grown in a T-25 flask (Nunc; Naperville, IL) were treated with ANP and incubated further for the indicated interval. The cell lysates were prepared and blotted as in our previous report (36).

Fluorescent immunocytochemistry. After treatment with ANP for 30 min, the colocalization of both phosphoprotein and nonphosphoprotein was observed after immunocytochemistry with double antibodies as described previously (36).

RESULTS

Low-dose ANP induces an increase in endothelial cell numbers. Low-dose ANP (10^{-11} mol/l) increased the cell numbers of HCAEC (52.5 ± 5.5%) and HUVEC (64.2 ± 11.4%), with the increase being observed in the range of 10^{-13}~10^{-11} mol/l ANP, whereas high doses (10^{-7}~10^{-5} mol/l) elicited a decrease in HCAEC (Fig. 1*A*). A low concentration of ANP also increased [^{3}H]thymidine incorporation, with the maximal increase being at 10^{-12} mol/l ANP (52.3 ± 12.2%). The increase in cell numbers induced by the low concentration of ANP became more prominent when a low concentration of serum was treated (Fig. 1*B*). We examined the effect of ANP on the change in the number of rat aortic smooth muscle cells cultured with 5% serum; 10^{-11} mol/l ANP did not affect the cell survival, whereas 10^{-5} mol/l ANP reduced the number of viable cells significantly (−24.6 ± 2.1%, $n = 6$). The following experiments were conducted using 10^{-11} mol/l ANP with 2% (for HCAEC) or 1% (for HUVEC) serum, which showed a prominent increase in cell numbers.

ANP-induced effects are dependent on cGMP and cGK. The basal cGMP concentration was 1.14 ± 0.25 fmol/2 × 10^4 cells. ANP (10^{-11} mol/l) increased the intracellular cGMP concentration fivefold over the basal level as early as 15 min after treatment. The increased cGMP content subsequently declined with incubation time, reaching the basal level at 12 h (Fig. 1*C*). A high dose of ANP (10^{-5} mol/l) greatly increased cGMP (77.4 ± 15.0-fold) at 15 min, followed by an abrupt decrease.

To test whether cGK is involved in the ANP-induced increase in cell numbers, the influence of cGK modulators was examined. A 2-day incubation of ANP also increased cell numbers, and the increase was completely blocked by 5 × 10^{-6} mol/l RP8 (15), a cGK inhibitor, in HUVEC (Fig. 1*D*) and HCAEC (data not shown). Similar to the biphasic response of ANP, a low concentration (10^{-11} mol/l) of SP8 (2, 15), a cGK agonist, increased cell numbers in both endothelial cell

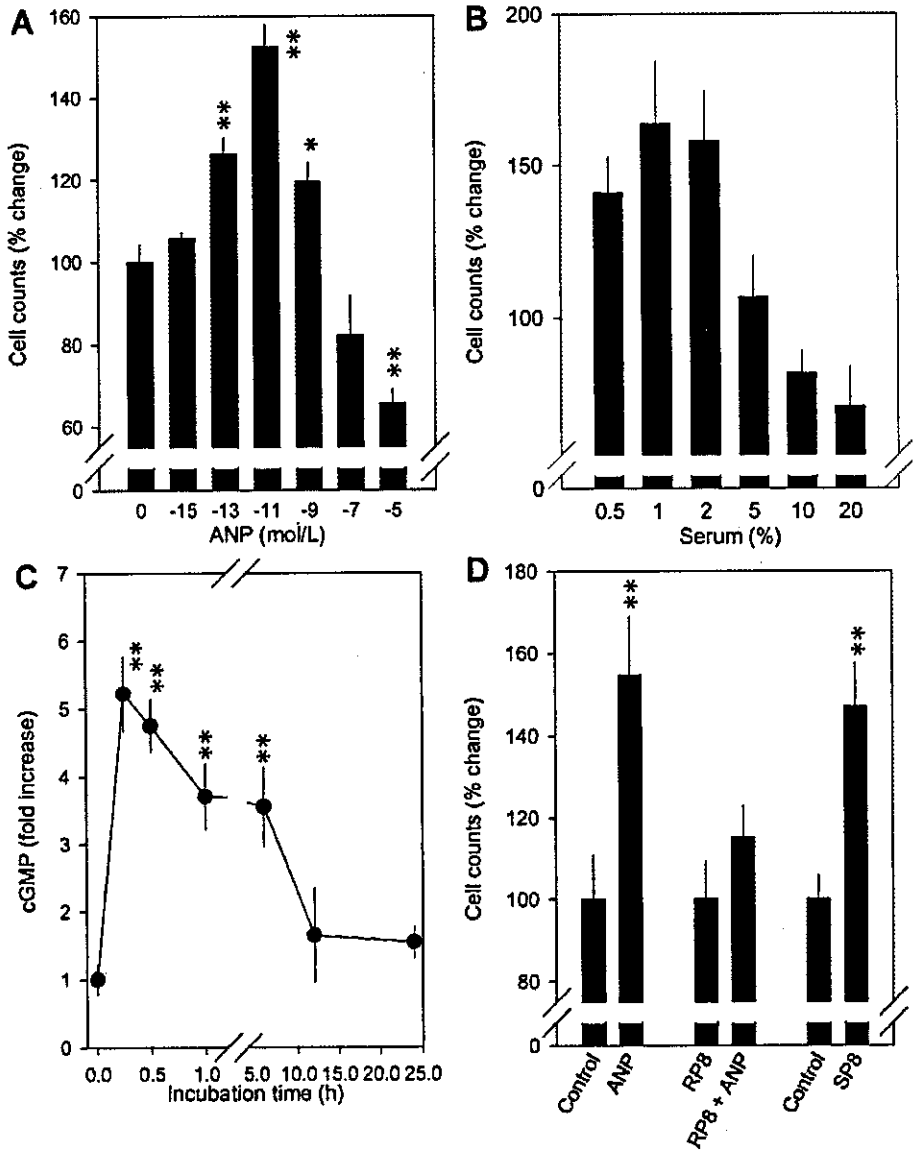

Fig. 1. Atrial natriuretic peptide (ANP)-induced increases in cell numbers and involvement of cGMP/cGMP-dependent protein kinase (cGK). *A*: effects of a 3-day incubation with varying doses of ANP on cell numbers in human coronary artery endothelial cells (HCAEC). *B*: relationship between varying concentrations of serum and ANP-induced increases in cell numbers in human umbilical vein endothelial cells (HUVEC). *C*: increases in cGMP induced by 10^{-11} mol/l ANP. *D*: effects of RP8-CPT-cGMP (RP8), a cGK inhibitor, on the increases in cell numbers induced by 10^{-11} mol/l ANP and of SP8-CPT- cGMPs (SP8), a cGK activator, in HUVEC. $^{*}P < 0.05$ and $^{**}P < 0.01$, significant differences from control.

types (Fig. 1*D*), whereas a high dose (10^{-5} mol/l) decreased the number by $-23.3 \pm 6.1\%$ (HCAEC) and $-35.2 \pm 13.0\%$ (HUVEC).

Protein kinases are involved in ANP-induced effects. We investigated the subsequent signal transduction pathway mediating the ANP-induced increase in endothelial cell numbers by pretreatment with the inhibitors of Akt, ERK1/2, and p38 MAPK (stress-activated protein kinase 2). Concentrations that minimally affected the basal cell number were selected (data not shown): 10^{-7} mol/l wortmannin, 10^{-5} mol/l PD-98059, and 5×10^{-6} mol/l SB-203580 (12, 15, 31, 45). Pretreatment with either wortmannin or PD-98059 significantly blocked the increase induced by 10^{-11} mol/l ANP, whereas the administration of SB-203580 showed no significant change (Fig. 2*A*). The inhibition induced by wortmannin or PD-98059 was dose dependent (Fig. 2, *B* and *C*).

Low-dose ANP provokes migration. First, we examined the effect of ANP on the migration with a conventional Transwell apparatus. Compared with the control, the numbers of HUVEC that migrated into the lower surfaces of the membranes increased in the ANP-treated group: 10^{-11} mol/l ANP increased cell

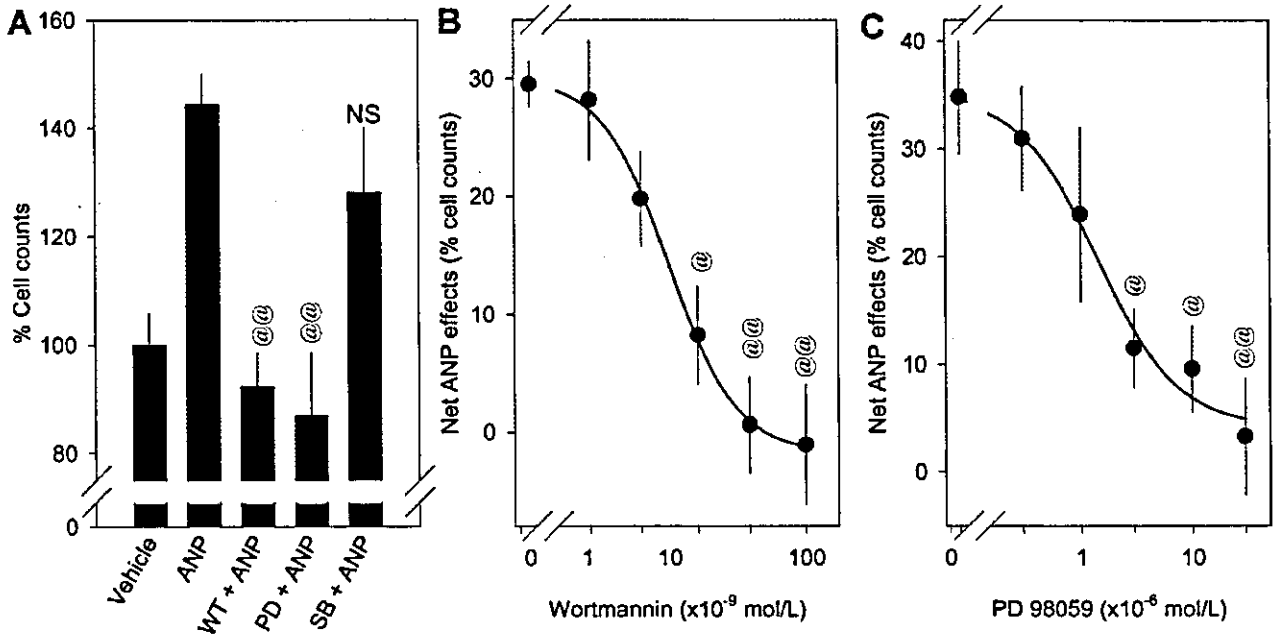

Fig. 2. Protein kinases and ANP-induced increases in cell numbers. *A*: effects of pretreatment with an Akt/PKB inhibitor [10^{-7} mol/l wortmannin (WT)], an ERK1/2 inhibitor [10^{-5} mol/l PD-98059 (PD)], and a p38 MAPK inhibitor [5×10^{-6} mol/l SB-203580 (SB)]. *B* and *C*: dose-dependent inhibition of WT (*B*) and PD (*C*). After treatment with various doses of inhibitors, ANP was administered and incubated for a further 2 days, the cell numbers were compared with those of inhibitor alone for each condition, and the net ANP effects over the "inhibitor-itself" basal were calculated as percent changes. @$P < 0.05$ and @@$P < 0.01$, significant differences from the ANP-treated group. NS, not significant.

migration by as much as 2.5 times ($P < 0.01$). bFGF, a positive control, increased migration ($P < 0.01$; Fig. 3*A*). Low-dose (10^{-11} mol/l) SP8 simulated the ANP effect (Fig. 3*A*). In contrast, pretreatment with RP8 blocked the increase in migration. Pretreatment with either wortmannin or PD-98059 significantly inhibited the migration. However, SB-203580 did not significantly affect migration (Fig. 3*B*).

Wound healing assay. In the wound healing assay, the total number of cells that migrated into the cell-

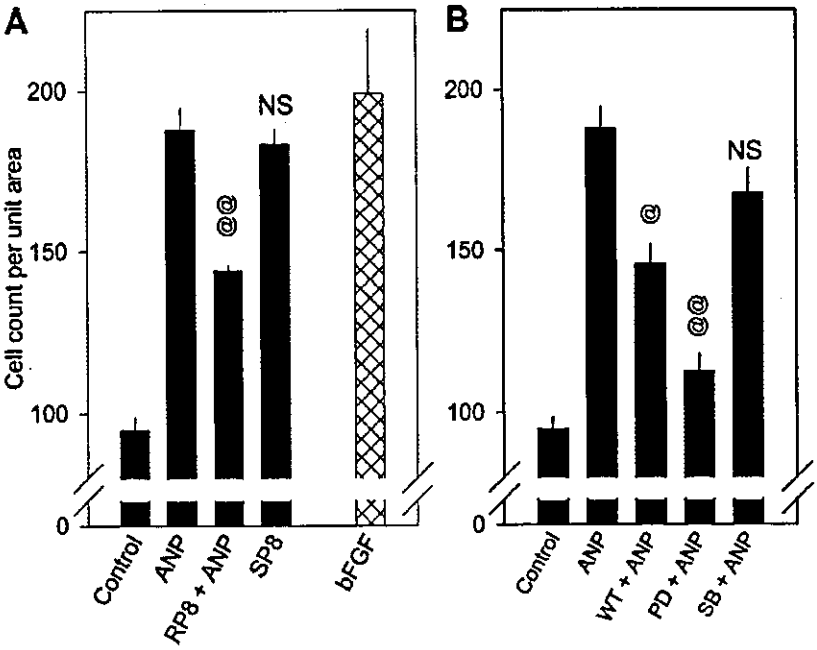

Fig. 3. Transwell migration test. *A*: effects of 10^{-11} M ANP on HUVEC migration and cGK modulator-induced changes in ANP effects. bFGF served as a positive control. *B*: effects of kinase inhibitors on the ANP-induced increases in migration. @$P < 0.05$ and @@$P < 0.01$, significant differences from the ANP-treated group.

free area 3 days after the wound was made was counted and plotted as shown in Fig. 4*A*. ANP (10^{-12} mol/l) increased the total number of migrated cells in the cell-free area.

The cells in the wound area could be divided into two different origins: cells that mainly migrated from the wound margin (migration component) and cells that mainly underwent mitosis (proliferation component). Therefore, we counted the cells in the small unit areas, plotted as seen in Fig. 4*B*, and calculated the *x*- and *y*-axis intercepts by extrapolation, which can represent, to a certain degree, the extent of migration and proliferation, respectively. ANP as well as 10 ng/ml VEGF significantly increased the migrating extent. The increase in migration induced by ANP was completely blocked by pretreatment with RP8 (Fig. 4*C*). ANP also significantly increased cell density at the starting point, a proliferating component, and, again, the increase was completely blocked by pretreatment with RP8 (Fig. 4*D*).

Pretreatment with either wortmannin or PD-98059 also attenuated the ANP-induced increase in total cell count (Fig. 5*A*). ANP-induced increases in the *x*-axis intercepts as well as the *y*-axis intercepts were blocked by pretreatment with either wortmannin or PD-98059. SB-203589 failed to block the ANP-induced increase in both intercepts (Fig. 5, *B*, *C*, and *D*).

Changes in actin arrangement. In untreated HUVEC, F-actin was found mostly in cortical structures (Fig. 6*A*). ANP produced reorganization of F-actin, characterized by the formation of long stress fibers that transversed the cells (Fig. 6*B*) and by the formation of membrane ruffling (Fig. 6*C*). However, the actin rearrangement was completely blocked by pretreatment with RP8 (Fig. 6*D*).

ANP induces phosphorylation of Akt and ERK1/2. After treatment with ANP, the contents of phospho-Akt and phospho-ERK1/2 were increased, and such increases were prominent within 1 h after treatment. However, the nonphosphorylated (total) Akt and ERK1/2 were unaltered by ANP treatment (Fig. 7, *A* and *B*).

Visualization of phospho-Akt and phospho-ERK1/2. In ANP-treated groups, some cells showed strong positive green fluorescence with phospho-Akt (Fig. 7*G*), whereas red fluorescence indicating Akt was not significantly altered (Fig. 7*H*), implying an increase in cell

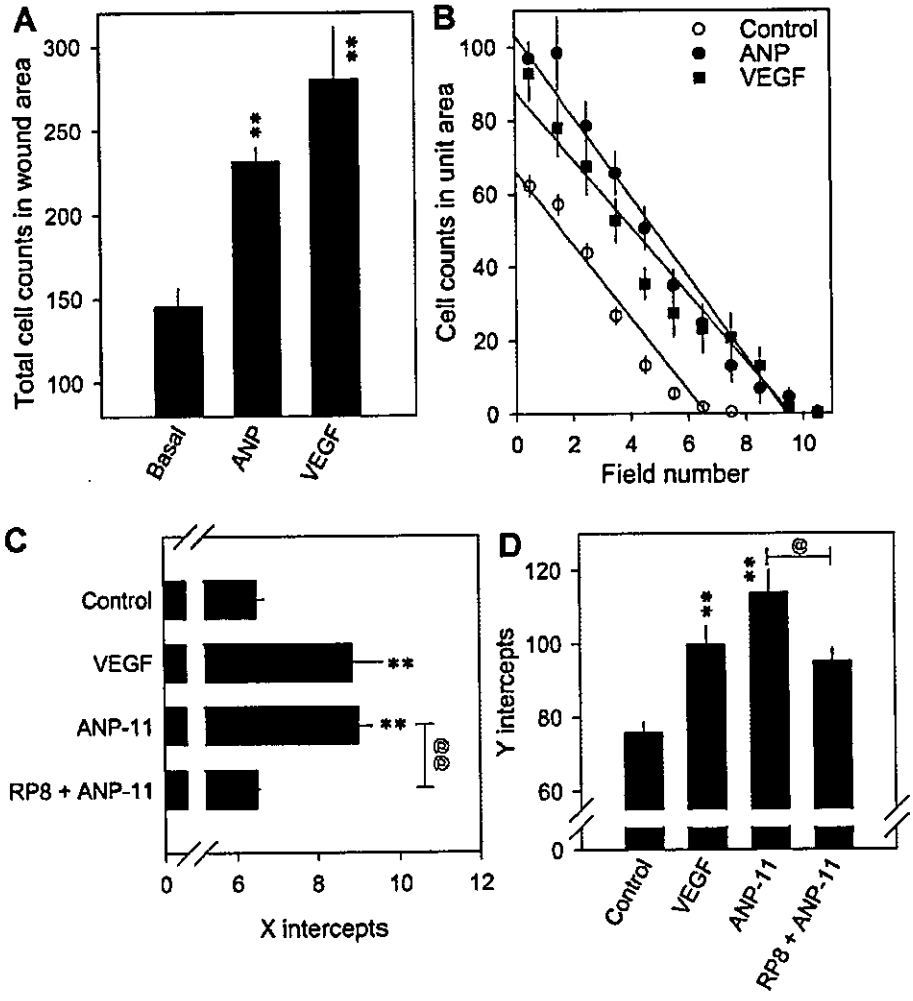

Fig. 4. The wound healing assay and its interpretation showing the proliferation and migration phases of migrated cells. *A*: total cell numbers that migrated into the cell-free area 3 days after the wound was made. VEGF served as a positive control. *B*: cell counts in consecutive areas from the wound margin. The cell numbers in each unit area were counted, plotted, and extrapolated to divide the migration component (*x*-axis intercepts) and proliferation component (*y*-axis intercepts). *C*: *x*-axis intercepts obtained from *B*, which show the extent of migration of cells. *D*: *y*-axis intercepts, which indicate virtual cell densities at the wound starting points. Values are means ± SE from 9 cases. $^{**}P < 0.01$, significant difference from control; $@P < 0.05$ and $@@P < 0.01$, significant differences from the ANP-treated group.

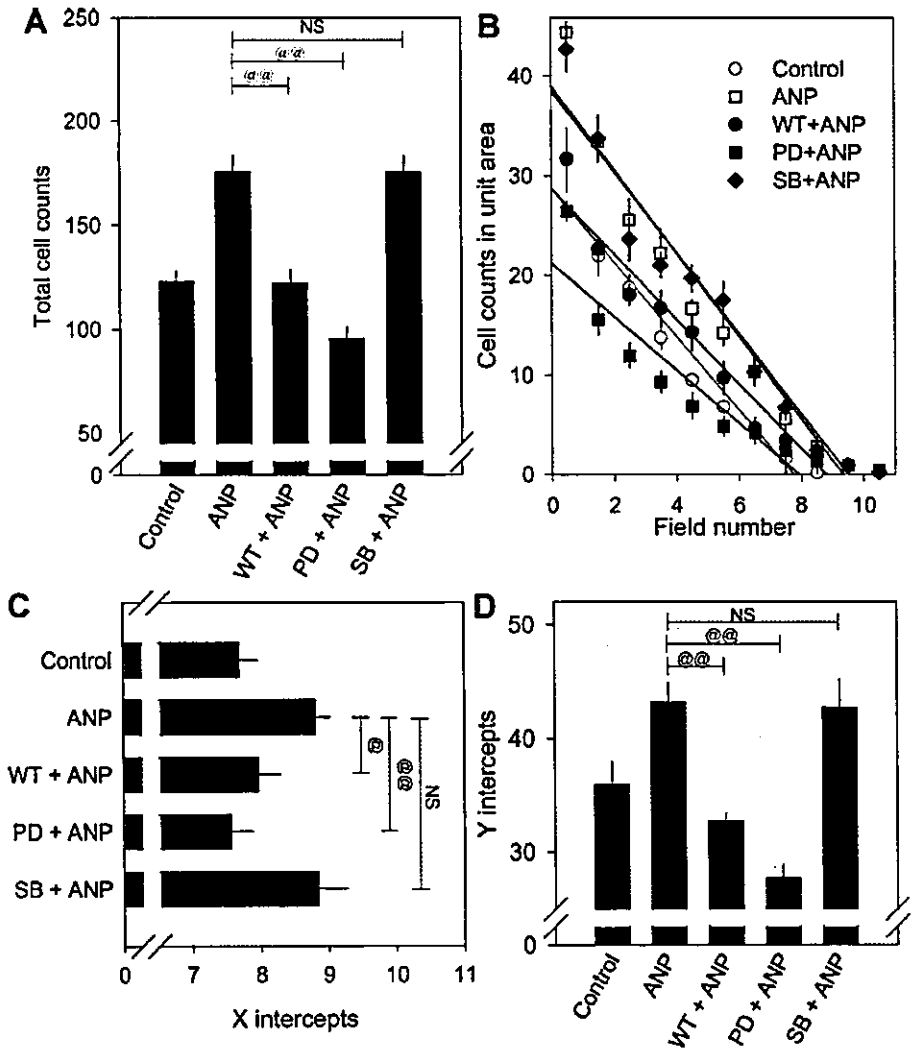

Fig. 5. Wound healing assay showing the inhibitory effects of protein kinase inhibitors. After the wound was made, WT (10^{-7} mol/l), PD (10^{-5} mol/l), and SB (5×10^{-6} mol/l) were administered. *A*: total cell counts in the cell-free area. *B*: cell counts in consecutive unit areas. *C*: *x*-axis intercepts. *D*: *y*-axis intercepts. @$P < 0.05$ and @@$P < 0.01$, significant differences from the ANP-treated group.

numbers with phosphorylated Akt. ANP also increased the phosphorylation of ERK1/2 (Fig. 7*M*).

DISCUSSION

This study documents a novel role of ANP in promoting endothelial regeneration. We showed that migration, as well as the number of endothelial cells, is increased by a low concentration of ANP and that both Akt and ERK1/2 pathways play principal roles in the signal transduction of ANP effects. We used a wound healing assay as an in vitro experimental model, and the results were consistent with our previous observations: that natriuretic peptides induce reendothelialization in an experimental animal model (6).

A series of studies have revealed that NO is a key molecule that induces vascular endothelial cell growth (46) and that it mediates VEGF-induced endothelial cell proliferation and migration (27). It has been proposed that increased cGMP, a downstream molecule of NO signal transduction, and subsequently activated cGK mediate the VEGF-induced MAPK activation in endothelial cells (15, 31). Thus the evidence that the cGMP/cGK system is related to vascular endothelial cell proliferation and migration raises the possibility that natriuretic peptides can possess similar potency on endothelial cells, because they share the same intracellular signal transduction pathway as NO.

In the present study, especially when the lower concentration of ANP within the physiological range (28, 40) was added, ANP increased cell numbers as well as DNA synthesis, suggesting the increase in cell numbers is caused by proliferation in part, although other mechanisms, such as the inhibition of apoptosis, may be involved simultaneously. In addition, the physiological concentration of ANP increased cell migration in both a Transwell migration test and wound healing assay. To our knowledge, this is the first demonstration of a natriuretic peptide-induced increase in cell numbers and migration in cultured human endothelial cells in an in vitro model, although one report mentioned that natriuretic peptide is associated with a higher cell growth rate in bovine bone endothelial cells (4).

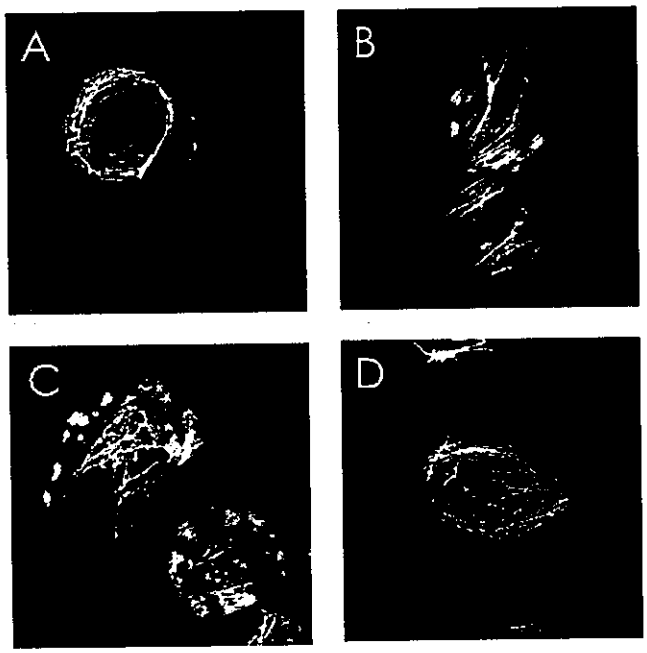

Fig. 6. ANP-induced stress fiber formation. After treatment with ANP, F-actin was stained with Alexa fluor 488-conjugated phalloidin and visualized with confocal laser scanning microscopy. *A*: control. *B* and *C*: ANP-treated cells. *D*: RP8-pretreated cells.

We further studied whether the ANP-induced effects were related to the increase in intracellular cGMP and subsequently activated cGK by pretreatment with RP8, a cGK inhibitor. Not only the production of cGMP was increased by low-dose ANP but also the increased migration and proliferation of the endothelial cells were blocked by RP8. Furthermore, SP8, a cGK activator, simulated the ANP effects to increase the number of viable cells and migration. These results are well correlated with increased intracellular cGMP and with the activation of cGK and strongly suggest that cGMP and cGK are involved in the ANP effects, although there might be mechanisms other than cGMP/cGK.

In the present study, ANP showed a typical bell-shaped response in the increase in cell numbers and migration, and the cGMP analog also induced biphasic changes: an increase with low doses but a decrease with high doses. High concentrations of ANP did not increase cell numbers, even though an increase in cGMP became much more prominent. It has been repeatedly shown that the effects of many growth factors do not follow a dose-dependent sigmoidal curve but a bell-shaped response, although the mechanism is not fully understood (14, 29, 30, 32). In endothelial cells, many growth factors also induced migration (25, 35) and proliferation (42) in a bell-shaped fashion. Thus ANP also seems to follow the same pattern of growth factors in inducing an increase in cell numbers at a lower concentration, whereas a decrease at a higher concentration is shown.

Early studies, including our own report, have shown that natriuretic peptides inhibit cell growth in the endothelial cell obtained from rats (16) and bovines (18). However, in those studies, the experimental conditions differed from ours in several points: the higher concentration of natriuretic peptides, different serum concentration, phenotypic alteration by subculture (39), and the species of animals employed. In those reports that showed growth arrest by natriuretic peptides, an inhibitory effect was observed at high concentrations of natriuretic peptide, such as 10^{-8}~10^{-6} mol/l. In our present study, we also observed a decrease in cell numbers at such concentrations. Considering that these concentrations are much higher than physiological conditions, as we reported (28, 40), the inhibitory response of cell growth does not seem to be of physiological significance. Moreover, their experiments were performed with a relatively high concentration of serum, which might have caused masking of the ANP-induced cell proliferation. We observed an increase in cell numbers only in groups treated with a low concentration of serum (<5%) without any growth factors included. Increasing the serum concentration abruptly decreased the ANP-induced increase in cell numbers. These observations suggest that the effects of proliferative stimuli could be dampened by strong mitogens. A report that CNP reciprocally antagonizes the mitogenic signaling of serum in fibroblasts (3) supports our present data, showing that cell proliferation is prominent only at a low concentration of serum.

Cell migration by extracellular mitogenic signals has been shown to be associated with alteration of actin reorganization into stress fibers (34, 41). Actin reorganization is characterized by the formation of lamellipodia, a transverse arrangement of stress fibers, membrane ruffling, and a forward extension in direction of movement (37). We found that ANP mediates stress fiber formation, consistent with the results of increased migration. Stress fiber formation and increased migration were blocked by RP8, suggesting the involvement of cGK in ANP-induced endothelial cell motility. These results are quite opposite to previous reports in which the natriuretic peptide family inhibits serum-induced endothelial cell migration (16) and lipid-induced vascular smooth muscle cell migration (20). However, as described above, they observed the effects at higher concentrations of natriuretic peptides than ours and under mitogen-stimulated conditions.

Members of the MAPK family, including ERK1/2 and p38 MAPK, are important mediators of signal transduction generated by growth factors, cytokines, and stressing agents, thereby regulating cellular growth and migration (33). ERK1/2 stimulates several factors, c-Fos, Elk-1, etc., thereby initiating DNA synthesis and proliferation (44). Another protein kinase, serine/threonin protein kinase Akt/PKB, which is activated by phosphoinositide 3′-kinase (11), is increasingly recognized as a key regulator of cell growth and migration (8, 19). The involvement of the Akt signaling pathway in endothelial cell proliferation and migration has also been elucidated (12, 26). p38 MAPK, also referred as stress-activated protein kinase 2, mediates actin reorganization and cell migration in human endothelial

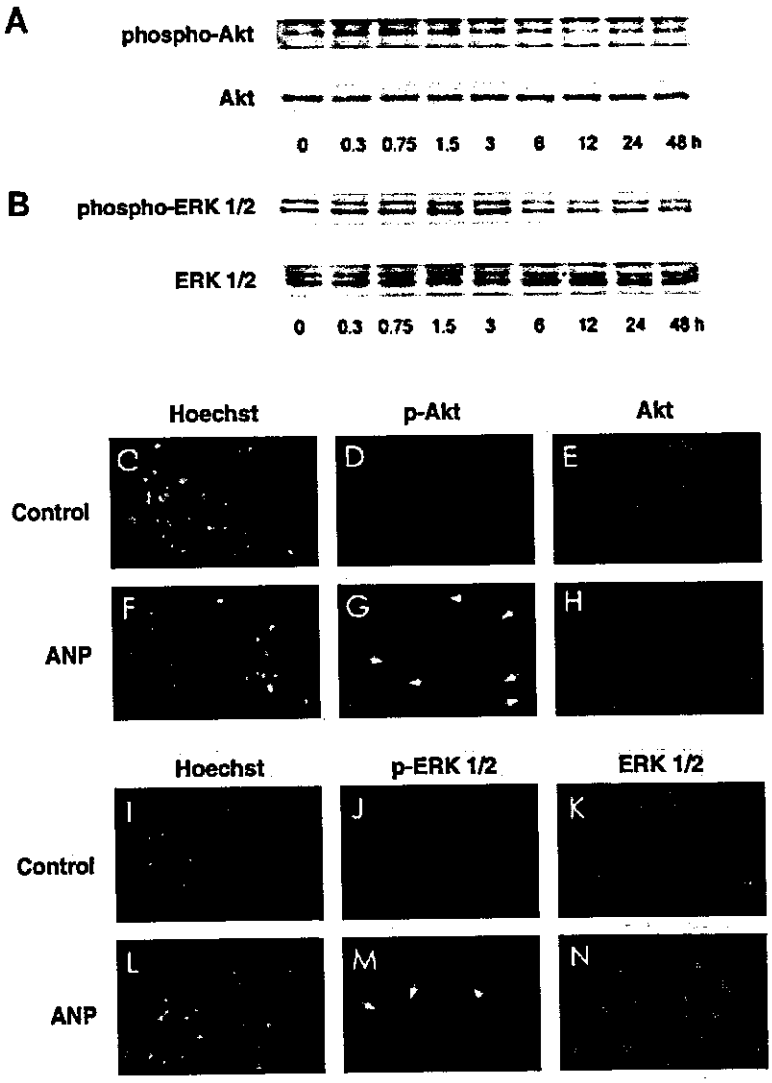

Fig. 7. *A* and *B*: Western blot analysis showing the quantitative changes of phospho-Akt (p-Akt) and phospho-ERK1/2 (p-ERK). ANP-treated cells were harvested at the indicated times, and the phosphoprotein contents were measured by immunoblots. *A*, *top*: typical immunoblots of phospho-Akt; *bottom*, total Akt. *B*, *top*: phospho-ERK1/2; *bottom*, total Erk. Typical blots from 3 independent experiments are shown. *C–N*: visualization of both phospho-protein kinase and total protein kinase at the same fields. *C*, *F*, *I*, and *L*: Hoechst 33342 staining for visualization of the nucleus. *D* and *G*: phospho-Akt stained with a specific monoclonal antibody and Alexa fluor 488-conjugated anti-mouse IgG antibody. *E*, *H*, *K*, and *N*: total Akt (*E* and *H*) and total ERK1/2 (*K* and *N*) stained with a specific polyclonal antibody and Alexa fluor 568-conjugated anti-rabbit IgG antibody. *J* and *M*: phospho-ERK1/2 stained with a specific monoclonal antibody. In the ANP-treated group, cells with a strong positivity against phospho-Akt (*G*) and against phospho-ERK1/2 (*M*) were observed, as indicated by the arrows.

cells induced by mitogens such as VEGF (34) or by platelet-derived growth factor (25). Therefore, we explored the signal transduction pathways of the ANP-induced events, focusing on Akt, ERK1/2, and p38 MAPK as possible intracellular mechanisms. In the present study, we demonstrated that the ANP-induced increases in both cell number and migration were blocked by either wortmannin or PD-98059, suggesting the involvement of Akt and ERK1/2 pathways in the ANP effects. In addition, the protein contents of both phospho-Akt and phospho-ERK1/2 were significantly increased in the early phase of ANP treatment. However, p38 MAPK did not seem to be involved in the ANP-mediated endothelial cell migration. The early increases in these phosphoprotein contents, as well as the cGMP level, seemed to trigger proliferation.

Raf-1, an initiating molecule in growth factor-induced proliferation, might play a key role in mediating the ANP/cGMP/cGK signal to MAPK pathways, because cGK directly associates with the Raf-1 and thereby activates the cascade involving ERK1/2 in human endothelial cells (15). It has been clearly elucidated that Akt activates endothelial NO synthase by phosphorylation, resulting in the increase in cGMP (5, 13). Conversely, Li et al. (24) found that reagents increasing intracellular cGMP levels activate Akt in primary hepatocytes and that wortmannin completely inhibited cGMP-induced Akt activation. These results suggest that phosphatidylinositide 3′-kinase and Akt may be stimulated by cGMP, supporting our observations that activated cGK by ANP may play a role in endothelial cell growth through cytoprotective Akt pathways. Activated Akt also mediates the endothelial cell migration by forming stress fibers and by actin reorganization (26), implying that the increased migration induced by ANP in the present study is partly mediated by Akt.

In summary, we demonstrated that ANP increases both cell number and migration, that the effects are prominent with a physiological concentration of ANP, and that the resulting increase in cGMP and activated

cGK are responsible for the activation of Akt and ERK1/2 pathways. The finding that these ANP mediate endothelial cell proliferation and migration by activating Akt and ERK1/2 signal transduction identifies natriuretic peptides as a new target to modulate angiogenesis. In this context, natriuretic peptides or their downstream molecules may have interesting therapeutic potential for inducing endothelial regeneration after vascular injury.

The authors express thanks to Dr. Young Do Jung of the Department of Biochemistry, Chonnam National University Medical School, for critical comments.

H. Kook was supported by a grant from the Chonnam National University Research Institute of Medical Sciences.

REFERENCES

1. **Arnold F and West DC.** Angiogenesis in wound healing. *Pharmacol Ther* 52: 407–422, 1991.
2. **Ashur-Fabian O, Perl O, Lilling G, Fridkin M, and Gozes I.** SNV, a lipophilic superactive VIP analog, acts through cGMP to promote neuronal survival. *Peptides* 20: 629–633, 1999.
3. **Chrisman TD and Garbers DL.** Reciprocal antagonism coordinates C-type natriuretic peptide and mitogen-signaling pathways in fibroblasts. *J Biol Chem* 274: 4293–4299, 1999.
4. **De Feo ML, Franceschelli F, Frediani U, Tosti-Guerra C, Crescioli C, Tanini A, Bartolini O, Becorpi A, Serio M, and Brandi ML.** Natriuretic hormone receptors and actions on bone endothelial cells. *Endocrinology* 133: 1759–1766, 1993.
5. **Dimmeler S, Fleming I, Fisslthaler B, Hermann C, Busse R, and Zeiher AM.** Activation of nitric oxide synthase in endothelial cells by Akt-dependent phosphorylation. *Nature* 399: 601–605, 1999.
6. **Doi K, Ikeda T, Itoh H, Ueyama K, Hosoda K, Ogawa Y, Yamashita J, Chun TH, Inoue M, Masatsugu K, Sawada N, Fukunaga Y, Saito T, Sone M, Yamahara K, Kook H, Komeda M, Ueda M, and Nakao K.** C-type natriuretic peptide induces redifferentiation of vascular smooth muscle cells with accelerated reendothelialization. *Arterioscler Thromb Vasc Biol* 21: 930–936, 2001.
7. **Doi K, Itoh H, Ikeda T, Hosoda K, Ogawa Y, Igaki T, Yamashita J, Chun TH, Inoue M, Masatsugu K, Matsuda K, Ohmori K, and Nakao K.** Adenovirus-mediated gene transfer of C-type natriuretic peptide causes G_1 growth inhibition of cultured vascular smooth muscle cells. *Biochem Biophys Res Commun* 239: 889–894, 1997.
8. **Dudek H, Datta SR, Franke TF, Birnbaum MJ, Yao R, Cooper GM, Segal RA, Kaplan DR, and Greenberg ME.** Regulation of neuronal survival by the serine-threonine protein kinase Akt. *Science* 275: 661–665, 1997.
9. **Ettenson DS and Gotlieb AI.** Centrosomes, microtubules, and microfilaments in the reendothelialization and remodeling of double-sided in vitro wounds. *Lab Invest* 66: 722–733, 1992.
10. **Folkman J.** Angiogenesis: initiation and control. *Ann NY Acad Sci* 401: 212–227, 1982.
11. **Franke TF, Kaplan DR, and Cantley LC.** PI3K: downstream AKT blocks apoptosis. *Cell* 88: 435–437, 1997.
12. **Fujio Y and Walsh K.** Akt mediates cytoprotection of endothelial cells by vascular endothelial growth factor in an anchorage-dependent manner. *J Biol Chem* 274: 16349–16354, 1999.
13. **Fulton D, Gratton JP, McCabe T, Fontana J, Fujio Y, Walsh K, Franke TF, Papapetropoulos A, and Sessa WC.** Regulation of endothelium-derived nitric oxide production by the protein kinase Akt. *Nature* 399: 597–601, 1999.
14. **Gruber BL, Marchese MJ, and Kew R.** Angiogenic factors stimulate mast-cell migration. *Blood* 86: 2488–2493, 1995.
15. **Hood J and Granger HJ.** Protein kinase G mediates vascular endothelial growth factor-induced Raf-1 activation and proliferation in human endothelial cells. *J Biol Chem* 273: 23504–23508, 1998.
16. **Ikeda M, Kohno M, and Takeda T.** Inhibition by cardiac natriuretic peptides of rat vascular endothelial cell migration. *Hypertension* 26: 401–405, 1995.
17. **Itoh H, Pratt RE, and Dzau VJ.** Atrial natriuretic polypeptide inhibits hypertrophy of vascular smooth muscle cells. *J Clin Invest* 86: 1690–1697, 1990.
18. **Itoh H, Pratt RE, Ohno M, and Dzau VJ.** Atrial natriuretic polypeptide as a novel antigrowth factor of endothelial cells. *Hypertension* 19: 758–761, 1992.
19. **Kauffmann-Zeh A, Rodriguez-Viciana P, Ulrich E, Gilbert C, Coffer P, Downward J, and Evan G.** Suppression of c-Myc-induced apoptosis by Ras signaling through PI (3)K and PKB. *Nature* 385: 544–548, 1997.
20. **Kohno M, Yokokawa K, Yasunari K, Kano H, Minami M, Ueda M, and Yoshikawa J.** Effect of natriuretic peptide family on the oxidized LDL-induced migration of human coronary artery smooth muscle cells. *Circ Res* 81: 585–590, 1997.
21. **Komatsu Y, Itoh H, Suga S, Ogawa Y, Hama N, Kishimoto I, Nakagawa O, Igaki T, Doi K, Yoshimasa T, and Nakao K.** Regulation of endothelial production of C-type natriuretic peptide in coculture with vascular smooth muscle cells. Role of the vascular natriuretic peptide system in vascular growth inhibition. *Circ Res* 78: 606–614, 1996.
22. **Komatsu Y, Nakao K, Itoh H, Suga S, Ogawa Y, and Imura H.** Vascular natriuretic peptide. *Lancet* 340: 622, 1992.
23. **Kook H, Rhee JH, Lee SE, Kang SY, Chung SS, Cho KW, and Baik YH.** Activation of particulate guanylyl cyclase by *Vibrio vulnificus* hemolysin. *Eur J Pharmacol* 365: 267–272, 1999.
24. **Li J, Yang S, and Billiar TR.** Cyclic nucleotides suppress tumor necrosis factor α-mediated apoptosis by inhibiting caspase activation and cytochrome c release in primary hepatocytes via a mechanism independent of Akt activation. *J Biol Chem* 275: 13026–13034, 2000.
25. **Matsumoto T, Yokote K, Tamura K, Takemoto M, Ueno H, Saito Y, and Mori S.** Platelet-derived growth factor activates p38 mitogen-activated protein kinase through a Ras-dependent pathway that is important for actin reorganization and cell migration. *J Biol Chem* 274: 13954–13960, 1999.
26. **Morales-Ruiz M, Fulton D, Sowa G, Languino LR, Fujio Y, Walsh K, and Sessa WC.** Vascular endothelial growth factor-stimulated actin reorganization and migration of endothelial cells is regulated via the serine/threonine kinase Akt. *Circ Res* 86: 892–896, 2000.
27. **Morbidelli L, Chang CH, Douglas JG, Granger HJ, Ledda G, and Ziche M.** Nitric oxide mediates mitogenic effects of VEGF on coronary venular endothelium. *Am J Physiol Heart Circ Physiol* 270: H411–H415, 1996.
28. **Mukoyama M, Nakao K, Hosoda K, Suga S, Saito Y, Ogawa Y, Shirakami G, Jougasaki M, Obata K, Yasue H, Kambayashi Y, Inouye K, and Imura H.** Brain natriuretic peptide as a novel cardiac hormone in humans. Evidence for an exquisite dual natriuretic peptide system, atrial natriuretic peptide and brain natriuretic peptide. *J Clin Invest* 87: 1402–1412, 1991.
29. **Ojaniemi M and Vuori K.** Epidermal growth factor modulates tyrosine phosphorylation of p130Cas. Involvement of phosphatidylinositol 3-kinase and actin cytoskeleton. *J Biol Chem* 272: 25993–25998, 1997.
30. **Okumura M, Okuda T, Nakamura T, and Yajima M.** Acceleration of wound healing in diabetic mice by basic fobroblast growth factor. *Biol Pharm Bull* 19: 530–535, 1996.
31. **Parenti A, Morbidelli L, Cui XL, Douglas JG, Hood JD, Granger HJ, Ledda F, and Ziche M.** Nitric oxide is an upstream signal of vascular endothelial growth factor-induced extracellular signal-regulated kinase1/2 activation in postcapillary endothelium. *J Biol Chem* 273: 4220–4226, 1998.
32. **Postel-Vinay MV, de Mello Coelho V, Gagnerault MC, and Dardenne M.** Growth hormone stimulates the proliferation of activated mouse T lymphocytes. *Endocrinology* 138: 1816–1820, 1997.
33. **Robinson MJ and Cobb MH.** Mitogen-activated protein kinase pathways. *Curr Opin Cell Biol* 9: 180–186, 1997.
34. **Rousseau S, Houle F, Kotanides H, Witte L, Waltenberger J, Landry J, and Huot J.** Vascular endothelial growth factor

(VEGF)-driven actin-based motility is mediated by VEGFR2 and requires concerted activation of stress-activated protein kinase 2 (SAPK2/p38) and geldanamycin-sensitive phosphorylation of focal adhesion kinase. *J Biol Chem* 275: 10661–10672, 2000.

35. **Rousseau S, Houle F, Landry J, and Huot J.** p38 MAP kinase activation by vascular endothelial growth factor mediates actin reorganization and cell migration in human endothelial cells. *Oncogene* 15: 2169–2177, 1997.
36. **Shin BA, Ahn KY, Kook H, Koh JT, Kang IC, Lee HC, and Kim KK.** Overexpressed human RAD50 exhibits cell death in a p21(WAF1/CIP1)-dependent manner: its potential utility in local gene therapy of tumor. *Cell Growth Differ* 12: 243–254, 2001.
37. **Stoker M and Gherardi E.** Regulation of cell movement: the motogenic cytokines. *Biochim Biophys Acta* 1072: 81–102, 1991.
38. **Suga S, Nakao K, Itoh H, Komatsu Y, Ogawa Y, Hama N, and Imura H.** Endothelial production of C-type natriuretic peptide and its marked augmentation by transforming growth factor-beta. Possible existence of "vascular natriuretic peptide system." *J Clin Invest* 90: 1145–1149, 1992.
39. **Suga S, Nakao K, Kishimoto I, Hosoda K, Mukoyama M, Arai H, Shirakami G, Ogawa Y, Komatsu Y, and Nakagawa O.** Phenotype-related alteration in expression of natriuretic peptide receptors in aortic smooth muscle cells. *Circ Res* 71: 34–39, 1992.
40. **Sugawara A, Nakao K, Morii N, Yamada T, Itoh H, Shiono S, Saito Y, Mukoyama M, Arai H, Nishimura K, Obata K, Yasue H, Ban T, and Imura H.** Synthesis of atrial natriuretic polypeptide in human failing hearts. Evidence for altered processing of atrial natriuretic polypeptide precursor and augmented synthesis of beta-human ANP. *J Clin Invest* 81: 1962–1970, 1988.
41. **Takaishi K, Sasaki T, Kato M, Yamochi W, Kuroda S, Nakamura T, Takeichi M, and Takai Y.** Involvement of Rho p21 small GTP-binding protein and its regulator in the HGF-induced cell motility. *Oncogene* 9: 273–279, 1994.
42. **Villablanca AC, Murphy CJ, and Reid TW.** Growth-promoting effects of substance P on endothelial cells in vitro. Synergism with calcitonin gene-related peptide, insulin, and plasma factors. *Circ Res* 75: 1113–1120, 1994.
43. **Von der Leyen, Gibbons G.F, Morishita R, Lewis NP, Zhang L, Nakajima M, Kaneda Y, Cooke JP, and Dzau VJ.** Gene therapy inhibiting neointimal vascular lesion: in vivo transfer of endothelial cell nitric oxide synthase gene. *Proc Natl Acad Sci USA* 92: 1137–1141, 1995.
44. **Whitmarsh AJ and Davis RJ.** Thranscription factor AP-1 regulation by migoten-activated protein kinase signal gransduction pathways. *J Mol Med* 74: 589–607, 1996.
45. **Xiong S, Grijalva R, Zhang L, Nguyen NT, Pisters PW, Pollock RE, and Yu D.** Up-regulation of vascular endothelial growth factor in breast cancer cells by the heregulin-beta1-activated p38 signaling pathway enhances endothelial cell migration. *Cancer Res* 61: 1727–1732, 2001.
46. **Ziche M, Morbidelli L, Masini E, Amerini S, Granger HJ, Maggi CA, Geppetti P, and Ledda F.** Nitric oxide mediates angiogenesis in vivo and endothelial cell growth and migration in vitro promoted by substance P. *J Clin Invest* 94: 2036–2044, 1994.

Available online at www.sciencedirect.com
SCIENCE DIRECT®
Regulatory Peptides 111 (2003) 13–19
REGULATORY PEPTIDES
www.elsevier.com/locate/regpep

Shear stress attenuates endothelin and endothelin-converting enzyme expression through oxidative stress

Ken Masatsugu, Hiroshi Itoh*, Tae-Haw Chun, Takatoshi Saito, Jun Yamashita, Kentaro Doi, Mayumi Inoue, Naoki Sawada, Yasutomo Fukunaga, Satsuki Sakaguchi, Masakatsu Sone, Kenichi Yamahara, Takami Yurugi, Kazuwa Nakao

Department of Medicine and Clinical Science, Kyoto University Graduate School of Medicine, 54 Shogoin Kawahara-cho, Sakyo-ku, Kyoto, 606-8507 Japan

Received 7 May 2002; received in revised form 12 September 2002; accepted 16 September 2002

Abstract

Shear stress is known to dilate blood vessels and exert an antiproliferative effect on vascular walls. These effects have partly been ascribed to shear stress-induced regulation of the secretion of endothelium-derived vasoactive substances. In this study, to elucidate the role of shear stress in endothelin production by endothelial cells, we examined the effect of physiological shear stress on the mRNA expression of endothelin-converting enzyme-1 (ECE-1) as well as endothelin-1 (ET-1) in cultured bovine carotid artery endothelial cells (BAECs) and human umbilical vein endothelial cells (HUVECs), using a parallel plate-type flow chamber.

ECE-1 mRNA expression was significantly down-regulated by shear stress in an intensity- and time-dependent manner within the physiological range (1.5 to 15 dyn/cm^2). ET-1 mRNA expression decreased together with ECE-1 mRNA expression. Shear stress at 15 dyn/cm^2 for 30 min induced a significant increase in the intracellular peroxide concentration, and the down-regulation of ECE-1 and ET-1 mRNA expression by shear stress was attenuated almost completely on treatment with *N*-acetyl cysteine (NAC), an antioxidant (20 mM). Furthermore, when H_2O_2 (0.5 to 2 mM) was added to BAECs in static culture, the ECE-1 as well as ET-1 mRNA expression was attenuated in proportion to the concentration of H_2O_2. It is suggested that endothelial cells sense shear stress as oxidative stress and transduce signal for the regulation of the gene expression of ECE as well as ET to attenuate vascular tone and inhibit the proliferation of vascular smooth muscle cells.

Keywords: Endothelial cells; mRNA; Flow; Hydrogen peroxide; Antioxidant; Angiotensin-converting enzyme

1. Introduction

Hemodynamic forces play an important role in the physiology and pathophysiology of hypertension and atherosclerosis. Shear stress is a mechanical force and key factor in the endothelium-dependent regulation of vascular tone and structure. Vascular endothelial cells sense shear stress and transduce signal for the transcriptional regulation of several sets of endothelial genes [1], so as to attenuate vascular tone and growth. In fact, it is known that the lower shear stress, the more atherosclerotic change [2].

We have studied the significance of vasoactive substances that play an important role in vascular tone and remodeling and reported that angiotensin II, a potent vasoconstrictor, promotes vascular growth [3]. Endothelin (ET) is also known to promote vascular growth. In contrast, the natriuretic peptides including atrial natriuretic peptide (ANP), brain natriuretic peptide (BNP) and C-type natriuretic peptide (CNP) inhibit vascular growth [4]. Our group has also demonstrated that CNP is produced and secreted from vascular endothelial cells to act as a novel endothelium-derived relaxing peptide (EDRP) [5]. Previously, we showed that CNP mRNA and secretion are augmented by shear stress [6]. Furthermore, we have reported that the expression of adrenomedullin (AM), which was originally isolated from pheochromocytoma tissues [7] and has been recently recognized as another EDRP [8], is also induced by shear stress [6].

The expression of ET-1, however, has been reported to be decreased by shear stress [9]. To form ET-1, big ET-1 has to be cleaved at Trp21-Val/Ile22, and an endopeptidase specific for this cleavage has been identified. cDNAs coding for two endothelin-converting enzymes (ECEs) have been

* Corresponding author. Tel.: +81-75-751-3170; fax: +81-75-771-9452.
E-mail address: hiito@kuhp.kyoto-u.ac.jp (H. Itoh).

0167-0115/02/$ - see front matter © 2002 Elsevier Science B.V. All rights reserved.
PII: S0167-0115(02)00219-7

Table 1
Primers and internal probes for reverse transcription-polymerase chain reaction/Southern blot analysis used in the present study

Primers		Oligonucleotide sequence
Human	sense	5′ CAG ATG CCT GCT CAA CAA CT 3′
ECE-1*	antisense	5′ TGC TGT CCT CGG CGA AGG TT 3′
Human	sense	5′ GCT GTT CCT TTC CTG GAT TA 3′
ECE-1a	antisense	5′ CAG TCC TGC CGC CAG AAG TA 3′
Bovine	sense	5′ CAA GCA GGA AAA GAA CTC AG 3′
ET-1	antisense	5′ AAA GAT GTT TTG ATG CTG TT 3′
Bovine	sense	5′ CAA ATG CCT GCT GAA CAA CT 3′
ECE-1	antisense	5′ TGC TGT CCT CAG CGA AGG TC 3′
	internal probe	5′ CGC TTC CAG GAC GCC GAC GA 3′
GAPDH**	sense	5′ ACC ACA GTC CAT GCC ATC AC 3′
	antisense	5′ TCC ACC ACC CTG TTG CTG TA 3′
	internal probe	5′ ACG GGA AGC TCA CTG GCA TG 3′

*The primer is common for ECE-1a and ECE-1b.
**The sequence of this probe is common for the human and bovine.

recently isolated, and the corresponding proteins have been named ECE-1 [10] and ECE-2 [11]. Both enzymes are membrane zinc-binding metalloendopeptidases. ECE-1 is mostly found in the plasma membrane [12], whereas ECE-2 is expressed mainly within the cell. Furthermore, the cloning of two human ECE-1 isoforms has been reported, and these two enzymes, referred to as ECE-1a and ECE-1b, differ in their *N*-terminus [13]. ECE-1a and ECE-1b mRNA are widely expressed in a variety of tissues, but ECE-1a is reported to be expressed more than ECE-1b in endothelial cells [14]. To further illustrate the involvement of ECE-1 in the regulation of vascular tone and structure and its relevance to the pathophysiology of hypertension and atherosclerosis, we examined the effect of physiological shear stress on ECE-1mRNA expression in cultured mammalian endothelial cells.

Recently, the production of intracellular reactive oxygen species (ROS) induced by shear stress has been reported and the involvement of oxidative stress in shear stress-induced signal transduction has been demonstrated [15]. So we further analyzed the involvement of oxidative stress in shear stress-induced down-regulation of ECE-1 and ET-1 mRNA expression.

2. Materials and methods

2.1. Cell culture

Primary bovine carotid artery endothelial cells (BAECs) [5] and human umbilical vein endothelial cells (HUVECs) were isolated as previously reported [6]. BAECs were cultured in medium-199 containing 10% fetal bovine serum.

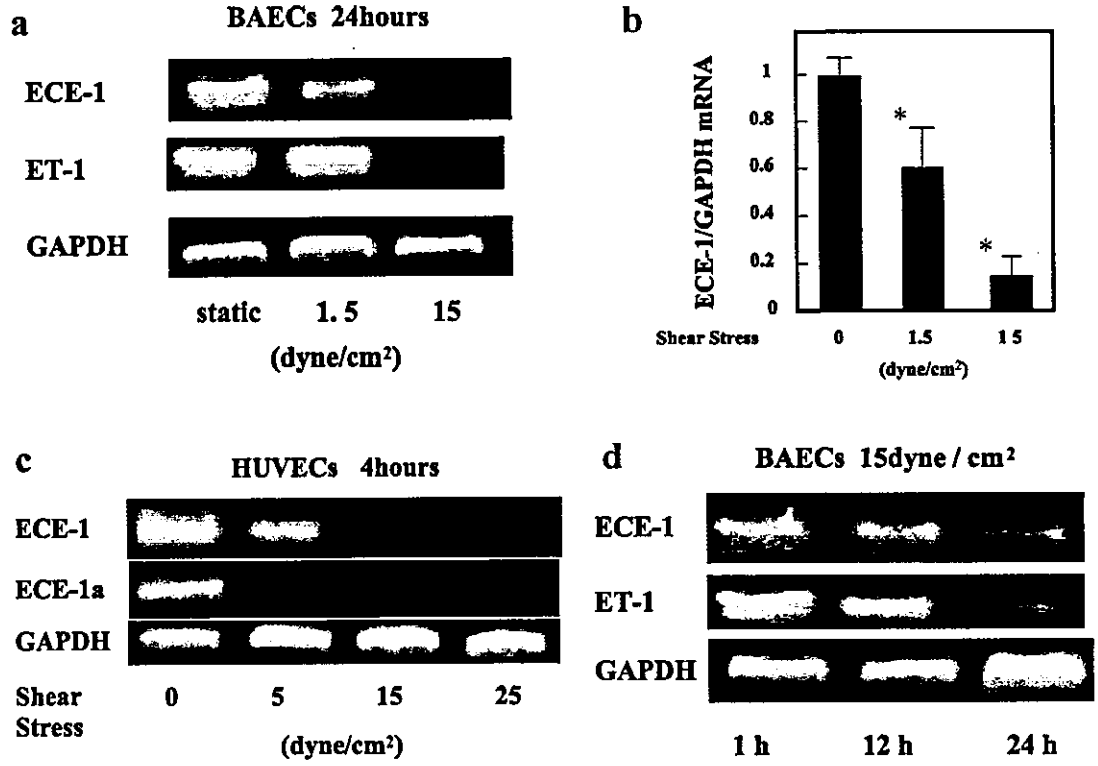

Fig. 1. Effect of shear stress on ET-1 and ECE-1 mRNA expression. (a) RT-PCR analysis of the intensity-dependent effect of shear stress on ECE-1 and ET-1 mRNA expressions in BAECs for 24 h. (b) Semiquantification with Southern blotting of the relative ratio of ECE-1 to GAPDH mRNA in BAECs in the static condition and with shear stress of 1.5 and 15 dyn/cm^2 for 24 h *$P < 0.05$. (c) RT-PCR analysis of the effect of shear stress (5–25 dyn/cm^2) on ECE-1 and ECE-1a mRNA expressions in HUVECs for 4 h. (d) RT-PCR analysis of ECE-1 and ET-1 mRNA expressions under a shear stress of 15 dyn/cm^2 from 1 to 24 h after loading.

Table 2
Time course of the effect of shear stress on big ET-1 and ET-1 concentrations in the culture media

Shear stress	Time	4 h	8 h	12 h
1.5 dyn/cm^2	big ET-1 (pg/ml)	222.0 ± 16.6	362.6 ± 69.0	424.2 ± 80.1
	ET-1 (pg/ml)	121.5 ± 31.1	165.1 ± 45.9	186.1 ± 27.2
15 dyn/cm^2	big ET-1 (pg/ml)	212.5 ± 6.3	262.2 ± 46.7*	219.0 ± 84.2*
	ET-1 (pg/ml)	109.3 ± 40.9	122.5 ± 65.1*	112.0 ± 31.4*

*$P<0.05$ vs. 1.5 dyn/cm^2.

HUVECs were grown in medium-199 (Dainippon Pharmaceutical) supplemented with 10% fetal bovine serum (Cell Culture Laboratories), 2 mmol/l L-glutamine and 100 μg heparin/ml.

2.2. Flow-loading apparatus

To apply a well-defined laminar flow, we used a parallel plate-type flow chamber as previously described [6]. Briefly, endothelial cells grown on glass plates were subjected to a constant laminar flow in a flow path 5.5×10^{-2}-m wide, 8.5×10^{-2}-m long, and 0.02×10^{-2}-m high. Shear stress intensity (dyn/cm^2 = 10^{-1} Pa [N/m^2])was calculated by the formula $\tau = 6\mu Q/ab^2$, where μ is the viscosity of the medium, Q is the flow volume (milliliters per second), a is the width of the flow path, and b is the height. Flow-loading experiments were performed at 37 °C and 5% CO_2 in a humidified incubator as we previously reported [6].

2.3. Reverse transcription-polymerase chain reaction and Southern blot analysis

Total cellular RNA was isolated from endothelial cells immediately after cessation of flow loading by the guanidinium, thiocyanate/phenol/chloroform extraction method, and treated with RQ-1 RNase-free DNAse (Promega). Reverse transcription into cDNA was carried out with 2 μg of total RNA in a 20-μl reaction volume with 0.5-μg Oligo (dT) 15 Primer (Promega) and 200 U SuperScript II RNaseH reverse transcriptase (Life Technologies) following the manufacturer's protocol. Polymerase chain reaction (PCR) was carried out with 2 μl of cDNA in a100-μl reaction volume containing 10 mmol/l Tris–Cl (pH 8.3), 50 mmol/l KCl, 4 mmol/l $MgCl_2$, 100 μmol/l primers, 200 μmol/l dNTP mix and 0.5 U Taq DNA polymerase (Takara Shuzo). Sense and antisense primers for bovine ECE-1, and human ECE-1 and ECE-1a (Table 1) were synthesized. Pairs of common PCR primers for human, bovine and rat glyceraldehyde 3-phosphate dehydrogenase (GAPDH) were purchased (Clontech Laboratories.). The temperature for amplification with a DNA Thermal Cycler (Perkin-Elmer

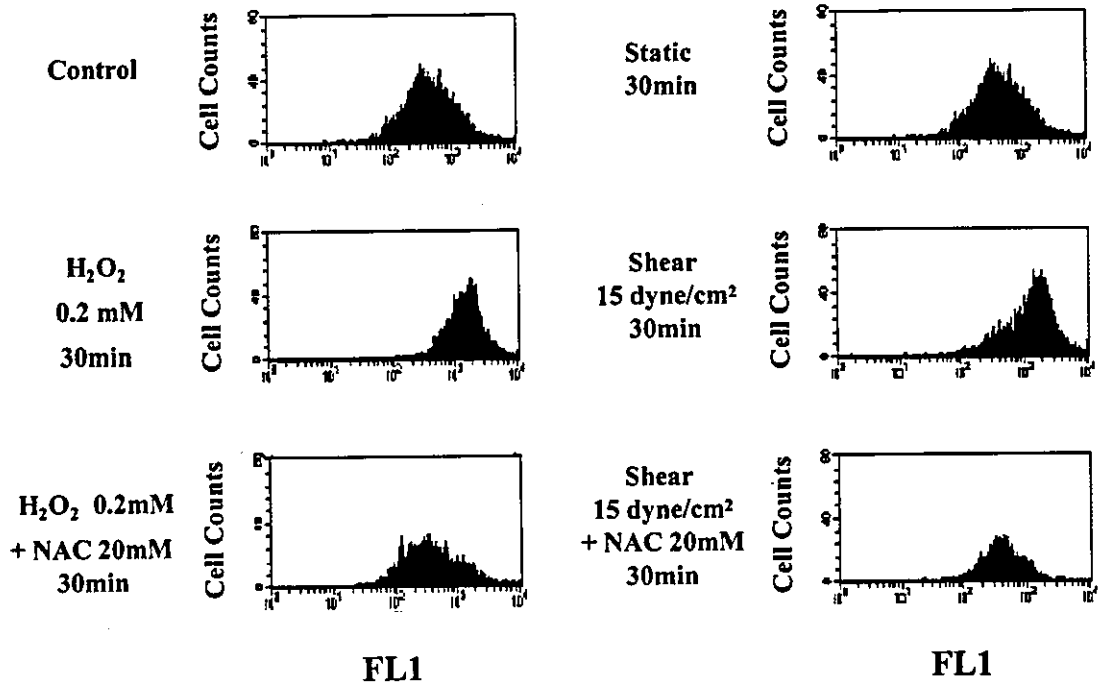

Fig. 2. Shear stress-induced intracellular ROS generation. Flow cytofluorometer histograms of relative fluorescence intensity after DCFH-DA loading in BAECs before H_2O_2 or shear stress-loading (control), incubated in the static condition for 30 min (Static 30 min), and 30 min after H_2O_2 (0.2 mM) administration (H_2O_2 0.2 mM 30 min), shear stress (15 dyn/cm^2) loading (Shear 15 dyn/cm^2 30 min), co-administration of H_2O_2 (0.2 mM) and *N*-acetyl cysteine (NAC) (20 mM) (H_2O_2 0.2 mM+NAC 20 mM 30 min) or shear stress (15 dyn/cm^2) loading with administration of NAC (20 mM) (shear 15 dyn/cm^2+NAC 20 mM 30 min).